Ocean acidification has different effects on the production of DMS and DMSP measured in cultures of *Emiliania huxleyi* and a mesocosm study: a comparison of laboratory monocultures and community interactions

Alison L. Webb[A]*, Gill Malin[A], Frances E. Hopkins[B], Kai Lam Ho[A], Ulf Riebesell[C], Kai G. Schulz[CE], Aud Larsen[D] and Peter S. Liss[A]

[A]Centre for Ocean and Atmospheric Sciences, School of Environmental Sciences, University of East Anglia, Norwich Research Park, Norwich, NR4 7TJ, U.K.
[B]Plymouth Marine Laboratory, Prospect Place, Plymouth, Devon PL1 3DH, U.K.
[C]GEOMAR Helmholtz Centre for Ocean Research Kiel, Düsternbrooker Weg 20, Kiel, Germany.
[D]Uni Research Environment, Thormøhlensgt. 49 B, N-5006 Bergen, Norway.
[E]Now at: Centre for Coastal Biogeochemistry, School of Environmental Science and Management, Southern Cross University, Lismore, NSW, Australia.

* Corresponding Author: Alison.l.webb@uea.ac.uk

Environmental Context

About 25% of CO_2 released into the atmosphere by human activities has been absorbed by the oceans, resulting in a process known as ocean acidification. This investigation focuses on the acidification effects on marine phytoplankton and subsequent production of the trace gas dimethylsulphide (DMS), a major route for sulphur transfer from the oceans to the atmosphere and the land. Increasing surface water pCO_2 has differential effects on the growth of different phytoplankton groups, and has resulted in varying responses in net community DMS production and therefore DMS release to the atmosphere.

Abstract

The human-induced rise in atmospheric carbon dioxide since the industrial revolution has led to increasing oceanic carbon uptake and changes in seawater carbonate chemistry, resulting in lowering of surface water pH. In this study we investigated the effect of increasing pCO_2 on concentrations of volatile biogenic dimethylsulphide (DMS) and its precursor dimethylsulphoniopropionate (DMSP), through monoculture studies and community pCO_2 perturbation. DMS is a climatically important gas produced by many marine algae: it transfers sulphur into the atmosphere and is a major influence on biogeochemical climate regulation through breakdown to sulphate and formation of subsequent cloud condensation nuclei (CCN). Overall, production of DMS and DMSP by the coccolithophore *Emiliania huxleyi* strain RCC1229 was unaffected by growth at 900 µatm pCO_2, but DMSP production normalised to cell volume was 12% lower at the higher pCO_2 treatment. These cultures were compared with community DMS and DMSP production during an elevated pCO_2 mesocosm experiment with the aim of studying *E. huxleyi* in the natural environment. Results contrasted with the culture experiments and showed reductions in community DMS and DMSP concentrations of up to 60% and 32% respectively at pCO_2 up to 3000 µatm, with changes attributed to poorer growth of DMSP-producing nanophytoplankton species, including

E. huxleyi, and potentially increased microbial consumption of DMS and dissolved DMSP at higher pCO_2. DMS and DMSP production differences between culture and community likely arise from pH affecting the inter-species responses between microbial producers and consumers.

Introduction

Since the 1750s, atmospheric carbon dioxide concentrations have increased from 280 to close to 400 µatm today due to anthropogenic inputs from burning fossil fuels, cement production and land use changes.[1] The atmospheric pCO_2 concentrations projected for 2100 are in the range 350 – 840 µatm; the majority of climate change scenarios project continuing increases over coming decades, with the possibility of decline through immediate change to low-carbon economies.[2] Approximately 25% of the total CO_2 emitted into the atmosphere by anthropogenic activities has been absorbed into the oceans to date, making the oceans a crucial sink for CO_2, with other sinks including the atmosphere (~45%) and land-based vegetation (~30%).[3] Dissolution of CO_2 in seawater results in the formation of carbonic acid, which readily dissociates to release H^+ and lower the pH, an effect termed 'ocean acidification'. Surface ocean pH levels will very likely be up to 0.4 units lower by 2100, a concomitant 150 % increase in H^+ ions, which will decrease the carbonate saturation state and result in increasing dissolution of calcium carbonate in surface waters.[4,5]

Emiliania huxleyi is a globally distributed haptophyte which produces calcite plates (coccoliths) covering the cell surface. Large-scale blooms of *E. huxleyi* occur in temperate shelf seas, including the North West European continental shelf in early summer,[6] and total global production of calcite by *E. huxleyi* makes it the most productive calcifying organism on Earth.[7] Under conditions of elevated pCO_2 in an ocean acidification scenario, calcite production by *E. huxleyi* has been found to typically decrease. [8,9] Calcium carbonate formation is a reaction that liberates CO_2 ($Ca^{2+} + 2HCO_3^- \rightarrow CaCO_3 + CO_2 + H_2O$), and any reduction in calcification rate can act as a negative feedback on rising surface water pCO_2.[10] Over longer timescales, calcite and organic carbon production by calcifying phytoplankton, and subsequent post-bloom settlement of this material through the water column is a major route for carbon transport from the surface oceans to storage in deeper waters.[11] Decreased surface pH could affect growth and subsequent calcite production and carbon fixation by *E. huxleyi* and have a significant impact on global cycling and removal of carbon in the future ocean.[8]

E. huxleyi is also a significant producer of dimethylsulphoniopropionate (DMSP), a compound produced by many phytoplankton species for several suggested purposes: as an osmoregulatory compound,[12] cryoprotectant,[13] anti-oxidant,[14] grazing defence[15] or chemoattractant.[16,17] DMSP is recognized as a significant part of the sulphur and carbon fluxes through marine microbial food webs, providing a reported 0.5 to 6 % of total carbon demand and between 3 and 100 % of total sulphur demand by marine bacteria[18] and major phytoplankton groups.[19] Breakdown of DMSP is a significant source of dimethylsulphide (DMS), a volatile compound released through the surface microlayer to the atmosphere where it oxidises to form sulphate-containing particles. These particles can

act as cloud condensation nuclei (CCN) in the troposphere, where cloud formation can reflect the Sun's energy back into space, with implications for global climate regulation.[20,21] The marine DMS-associated global sulphur flux to the atmosphere has been calculated at 28.1 Tg S per year.[22]

Previous community pCO_2 perturbation experiments in natural waters have identified changes in DMS and DMSP concentrations as pCO_2 increased.[23–28] Here we investigated the effects of elevated pCO_2 on DMS and DMSP production in a low-bacterial abundance monoculture of *E. huxleyi* (strain RCC1229), and progressed to investigate the effect of pCO_2 on a community known to contain a natural *E. huxleyi* population. The hypotheses of this investigation were that elevated pCO_2 would affect the physiology of the *E. huxleyi* cell and result in lower production of intracellular DMSP, which would result in lower DMS production. On a community level, elevated pCO_2 may stimulate primary productivity, resulting in increased community DMSP synthesis and higher DMSP concentrations.[29] In contrast, an increase in bacterial productivity at elevated pCO_2 would create a greater demand for sulphur and increase DMS and DMSP consumption.[30,31] This investigation aimed to determine if changes in DMS and DMSP concentrations under high pCO_2 are a result of physiological changes in the *E. huxleyi* cell, or changes in microbial inter-species responses to elevated pCO_2, nutrient competition and DMSP consumption.

Emiliania huxleyi **Culture Setup**

E. huxleyi strain RCC1229 was chosen for its high level of calcification and origin in the North Sea (as a strain isolated close to the location of the mesocosm experiment) and grown in autoclaved aged natural seawater medium enriched with ESAW (Enriched Seawater Artificial Water) nutrients (starting concentration 186.7 µmol L^{-1} NO_3 and 20.1 µmol L^{-1} PO_4) and vitamins.[32] The stock culture was treated for 2 days with a broad-spectrum antibiotic mixture[33] to significantly reduce bacterial abundance, before regular reinoculation into fresh medium to maintain exponential growth for 10 days prior to pCO_2 perturbation (day T0). All cultures were maintained at 15°C in a 16:8 light/dark cycle with light at 180 µmol photons m^{-1} s^{-1}.

Cells were grown in a semi-continuous culture, with three replicate cultures exposed to 900 µatm pCO_2 and three replicate control cultures treated with air at ambient pCO_2 (395 µatm) Prior to inoculation, the medium was filter sterilised, decanted into two bespoke vessels and pre-sparged to the pCO_2 treatment concentration using pre-prepared CO_2 gas mixtures (BOC Ltd, UK). Cultures were grown in 1 L Erlenmeyer flasks with 500 mL of pre-prepared sterile medium and sufficient inoculum to provide a starting cell count of 120,000 cells mL^{-1}. Cultures were grown over 4 day periods to cell densities of ca. 1,000,000 cells mL^{-1} before re-inoculation into fresh medium to keep the culture in exponential growth. Flasks were sealed with ground glass Quikfit stoppers modified to enable inlet and outlet gas lines. Aqueous phase bubbling of the cultures was avoided but the headspaces of each flask were flushed daily with the respective treatment gas for 10 minutes at a rate of 30 mL

min^{-1} through a 0.2 µm Minisart filter (Sartorius Ltd, Epsom, U.K.). Samples were extracted from the flasks through a luer-lock sealed opening in the base of the flask; to prevent contamination of the culture, all sampling from this outlet used sterile luer fittings on 25 mL glass syringes.

Measurement of Biological Parameters

Culture samples for cell volume, cell counts, pH, DMS and total DMSP ($DMSP_T$) were taken daily 7h after the onset of the light period. Cell volume and counts were measured in triplicate from live culture using a Coulter Multisizer III (Beckman Coulter Ltd, High Wycombe, U.K.). Average growth rates were determined for each inoculation period as $\ln(N_1/N_0)/(t_1 - t_0)$, with cell counts N_0 and N_1 taken at the time points t_0 and t_1 respectively. All six cultures were examined under x100 magnification using an Olympus BX40F-3 fluorescence microscope and no non-calcified cells could be identified from multiple prepared samples. For pH analysis, 20 mL of culture from each flask was analysed daily at 15°C by the standard potentiometric technique[34,35] using a Seven Easy S20 probe with automatic temperature adjustment (relative accuracy ±0.01 Mettler-Toledo Ltd, Beaumont Leys, U.K.) using NBS buffers.

DMS and DMSP Analysis

DMS samples were extracted by injection of 2mL of filtered culture into a PTFE purge and cryotrap system and purged with oxygen-free nitrogen (OFN) for 5 minutes at 80 mL min^{-1}. Samples were trapped in a PTFE sample loop suspended above liquid nitrogen and held at -150°C, before immersion in boiling water and injection into a Shimadzu GC2010 gas chromatograph (GC) with a Varian Chrompack CP-Sil-5CB column (30m, 0.53mm ID) and flame photometric detector (FPD). The GC was operated isothermally at 60°C and DMS eluted at 2.1 minutes; the GC was calibrated using liquid DMSP standards treated with 10M NaOH in the concentration range 5.07 – 406.2 nmol L^{-1} (7% analytical error through analysis of 10 samples). Six-point calibrations were performed weekly and checked daily for instrument drift, and the resulting calibrations typically produced linear regression with r^2 >0.99. The same method was used when participating in the AQA 12-23 international DMS analysis proficiency test in February 2013 and achieved close agreement with the concentration of the test material.[36]

Triplicate $DMSP_T$ samples from each flask were prepared in 4 mL headspace vials by the addition of 0.5 mL 1M NaOH to 3 mL of culture and sealed using PTFE screw caps and PTFE/ silicone septa. All DMSP vials were stored for 24 hours at 30°C before an MPS2 Twister multi-purpose autosampler (Gerstel, Mülheim, Germany) equipped with a 250 µL Hamilton syringe sampled 100 µL of headspace from each vial and injected it into the GC-FPD as set up above.

Mesocosm Experiment Setup

The experiment was performed at the Marine Biological Station at Espegrend, University of Bergen, Norway from 6th May to 12th June 2011, with nine cylindrical thermoplastic polyurethane (TPU) mesocosm enclosures (ca 75 m^3, 25m water depth) anchored approximately 100 m apart and 1 mile offshore in the Raunefjord (60.265°N, 5.205°E) at a water depth of 55 to 65m. Each enclosure was supported by an 8m tall floating frame and capped with a polyvinyl chloride (PVC) hood.[37] Over 95% of the incoming photosynthetically active radiation (PAR) was transmitted by the TPU and PVC materials, with near 100% absorbance of incoming UV radiation. The mesocosms were filled on the 1st May 2011 (day T-7) by lowering the bags through the CO_2 under-saturated post-bloom water column with the bottom openings covered with 3 mm mesh to exclude larger organisms. Full exclusion of the mesocosms from the surrounding waters occurred 3 days later: the lower opening was fitted with a sediment trap and the upper openings were raised above the water surface.[37]

The carbonate chemistry of the water was altered by the addition of CO_2-saturated, filtered fjord water to alter the dissolved inorganic carbon (DIC) concentrations while keeping alkalinity constant.[38] This water was added to 7 mesocosms depending on the target pCO_2 concentrations over a 5 day period, starting on the 8th May 2011 (day T0). This was done with a bespoke dispersal apparatus ('Spider') that was lowered through the bags to ensure even distribution of CO_2-rich waters throughout the water column. Two mesocosms were designated controls and received no addition of CO_2 enriched water (M2 and M4, 280 µatm). The range of target pCO_2 was 390 to 3000 µatm across the seven enriched mesocosms (M6, 390 µatm; M8, 560 µatm; M1, 840 µatm; M3, 1120 µatm; M5, 1400 µatm; M7, 2000 µatm; M9, 3000 µatm) taking into account IPCC projections up to the year 2300 and beyond,[2] in order to identify the change in different parameters to increasing pCO_2. pCO_2 and pH were calculated from the coulometric measurement of DIC[39] and spectrophotometric determination of pH[40] using the stoichiometric equilibrium constants for carbonic acid[41,42]. No further perturbation was made to the carbonate system once the experiment had commenced. Inorganic nutrients were added to each mesocosm on T14 to stimulate phytoplankton growth. The inside of the mesocosm walls was cleaned regularly with a ring-shaped, double-bladed wiper to prevent biofilm growth.[37] After termination of the experiment, one small hole was detected in the bag of M2 which had led to non-quantifiable water exchange, so the results from this mesocosm were removed from the analysis.

DMS and DMSP Extraction and Analysis

An integrated water sampler (IWS, Hydrobios GmbH, Kiel, Germany) was used every morning to collect samples from the full 25m water depth of all nine mesocosms. Samples for DMS and DMSP analysis were collected in an amber bottle from the laminar flow of the IWS using Tygon tubing and the bottle was allowed to overflow for twice the volume before the tube was removed and the glass stopper firmly inserted to prevent air bubbles and atmospheric contact. DMS samples (40 mL) were injected into a purge and cryotrap system[43] through a 25 mm Whatman GF/F (GE Healthcare Life Sciences, Little Chalfont, England) and were purged with oxygen-free nitrogen (OFN) at 80 mL min^{-1} for 10 minutes. Gas samples passed through a glass wool trap to remove aerosols and water

droplets, and a series of two nafion counterflow driers operating at 180 mL min^{-1}, before DMS was trapped in a stainless steel sample loop held above liquid nitrogen at -150°C.

DMS samples were injected into an Agilent 6890 gas chromatograph equipped with a 60m DB-VRX capillary column (0.32 mm ID, 1.8 µm film thickness, Agilent J&W Ltd) according to the programme outlined by Hopkins *et al.*[24] Analysis was by an Agilent 5973 quadrupole mass spectrometer operated in electron ionisation (EI), single ion mode (SIM), and was calibrated using a gravimetrically prepared liquid DMS standard diluted in HPLC-grade methanol to the required concentration in the range 0.04 – 7.64 nmol L^{-1} (10% analytical error for triplicate measurements). GC-MS Instrument drift was corrected using 2 µL of a diluted deuterated DMS (D_6-DMS) as a surrogate analyte.[44,45] Five-point calibrations were performed weekly, and checked daily, and the linear regression from the calibrations typically produced values r^2 >0.98.

$DMSP_T$ samples were prepared for later analysis using the acidification method of Curran *et al.*[46,47] by storing 7 mL of unfiltered aliquots of seawater in 8 mL glass sample vials (Labhut, Churcham, UK) with 0.35 µL of 50% H_2SO_4. All samples were stored in the dark at room temperature for 8 weeks prior to analysis. $DMSP_T$ was extracted by purging of 2 mL unfiltered sample with 1 mL 10M NaOH with OFN for 5 minutes at 80 ml min^{-1}, before analysis by GC-FPD as described above.

Additional Measurements

Water samples were collected from the IWS every first or second day, and phytoplankton abundances were determined with a FacsCalibur flow cytometer (Becton Dickinson) equipped with an air-cooled laser providing 15 mW at 488 nm with standard filter set-up. The counts were obtained from fresh samples with the trigger set on red. Discrimination of *Synechococcus* spp., *Emiliania huxleyi,* and autotrophic picoeukaryotes, cryptophytes and other autotrophic nanoeukaryotes was based on dot plots of side-scatter signal (SSC) versus pigment autofluorescence (Chlorophyll-*a* and phycoerythrin).[48]

For determination of chlorophyll-*a* (Chl-*a*) concentrations, aliquots of 250-500 mL of sample from the IWS were also filtered onto GF/F and stored frozen for 24 hours prior to homogenisation in 90% acetone with glass beads. The mixture was centrifuged at 800 x g and the Chl-*a* concentrations were determined on a Turner AU-10 fluorometer.[49] Further samples were extracted in 100 % acetone and analysed by high performance liquid chromatography (WATERS HPLC with a Varian Microsorb-MV 100-3 C8 column),[50] with phytoplankton community composition calculated using the CHEMTAX algorithm by converting the concentrations of marker pigments to the Chl-*a* equivalents.[51,52]

Statistical Analysis

Statistical analysis was performed using Minitab v16. All data were checked for normality using an Anderson – Darling test prior to statistical analysis, and were transformed where necessary. Equal variance was confirmed

using Levene's Tests. One-way ANOVA combined with Tukey's post analysis tests were used on the DMS and DMSP data to determine differences between the mesocosms at different pCO_2 concentrations. Spearman's Rank Correlation was also used to determine the relationships between pCO_2 and DMS and DMSP concentrations over the course of the experiment, as well as the relationships between different community variables and the trace gas concentrations. Two-tailed t-tests were used to determine differences between the control and CO_2 treatments during the laboratory studies.

E. huxleyi High pCO_2 Culture Experiment Results

Growth Parameters

pH within the CO_2 treatment cultures started at a mean of 7.43 immediately following inoculation compared to 7.90 in the air control (Figure 1a). As the culture grew, the pH gradually increased in all flasks, but in the CO_2 treatment cultures pH was significantly lower than for the air control ($T=7.68$, $p<0.01$), and re-inoculation reduced the pH in all cultures. Mean pH for the entire experiment was 7.72 in the CO_2 treatment and 8.13 in the control. Cultures from both treatments grew exponentially for four days after inoculations 1, 2 and 3, and for five days in the fourth and fifth inoculations. Cell counts at the end of each inoculation period ranged from 6.3×10^5 to 1.34×10^6 cells mL^{-1}, and there was no increase in cell count with elevated CO_2 (Figure 1b), with the average specific growth rate 0.47 d^{-1} in both treatments. Cell volume varied in *E. huxleyi* cultures so the data are presented as total cell volume (Figure 1c), and was used to calculate mean individual cell volume, which increased in the 900 µatm CO_2 treatment as the experiment progressed (Figure 1d). Mean cell volume in the control treatment was 46.0 ± 12.0 μm^3 and in the CO_2 treatment was 53.4 ± 13.8 μm^3, and cells showed a 20% increase in volume during the fifth inoculation compared to the control treatment ($T=-3.65$, $p<0.01$).

DMS and DMSP Dynamics

Aqueous DMS was measured daily (Figure 2a) alongside the cell count and volume analyses, and was normalised to cell number (Figure 2b). During the first two culture periods up to T9, DMS was in the range 6.5 – 65.1 nmol L^{-1}, but during the following three culture periods, DMS increased sequentially to higher concentrations up to a mean of 328.8 ± 56.1 nmol L^{-1} in the CO_2 treatment and 296.8 ± 69.2 nmol L^{-1} in the control at T23. DMS data normalised to cell volume showed no effect of CO_2 treatment on the DMS production ($T=0.77$, $p=0.444$) but was on average 80% lower in the first inoculation compared to the final inoculation period with a range of 0.6 – 11.5 mmol L^{-1} cell volume (CV).

$DMSP_T$ concentrations increased exponentially with cell count (Figure 2c) from a mean of 505.3 ± 118.7 nmol L^{-1} (control) and 504.9 ± 140.2 nmol L^{-1} (CO_2) in the initial days of inoculation to 4444.5 ± 1127.2 nmol L^{-1} (control)

and 4180.2 ± 1000.0 nmol L^{-1} (CO_2) on the final day of each inoculation. $DMSP_T$ normalised to cell volume varied over the course of the experiment, within the range 16.7 – 202.1 mmol L^{-1} cell volume (CV) and was 12% lower in the CO_2 treatment than the control over the entire experiment (Figure 2d; T=3.71, $p<0.01$, n=138). The measured DMS: $DMSP_T$ ratio was calculated (Figure 2e) with a mean of 0.04. The ratio had a sharp peak on T19 in both treatments, reaching a maximum of 0.23 in the CO_2 treatment, but over the course of the experiment, increased pCO_2 had no significant effect on the DMS: $DMSP_T$ ratio. A summary of the *E. huxleyi* culture results is given in Table 1.

Mesocosm Experiment Results

Changes in Physical Oceanographic Conditions

Inorganic nitrate and phosphate concentrations in the mesocosms were measured at 1.54 (±0.30) µmol L^{-1} and 0.21 (±0.01) µmol L^{-1} respectively on T-1 of the experiment, with addition of artificial inorganic nutrients to all mesocosms on T14 to stimulate phytoplankton growth (mean concentrations 5.0 ± 0.2 µmol L^{-1} NO_3 and 0.16 ± 0.02 µmol L^{-1} PO_4 after addition). Maximum nutrient concentrations measured in the fjord were 1.73 µmol L^{-1} NO_3 and 0.06 µmol L^{-1} PO_4. Outgassing of CO_2 and carbon fixation by phytoplankton caused a gradual pCO_2 decline and pH increase in CO_2-enriched mesocosms (Figure 3). The average pH before nutrient addition ranged between pH 8.13 ± 0.01 in the control mesocosms and pH 7.31 ± 0.12 in M9 (3000 µatm), the highest pCO_2 mesocosm. After nutrient addition, pH ranged between pH 8.14 ± 0.01 in the control mesocosms and pH 7.49 ± 0.05 in the highest pCO_2 mesocosm. Temperature varied between 6.8°C at the beginning and 10.0°C at the end of the experiment.

Changes in Community Composition

Three phases were identified from the fluorometric Chl-*a* data (Figure 4a): phase 1 as the initial bloom prior to artificial nutrient addition, phase 2 as the artificial nutrient-induced bloom and phase 3 as post-bloom. The initial Chl-*a* concentrations in all mesocosms were 2.2 ± 0.1 µg L^{-1} at T-1 and rapidly increased in a similar manner in all treatments during the phase 1 bloom (Figure 4a), peaking on T3 in all mesocosms except for M9 (3000 µatm) which continued to increase until 4.1 µg L^{-1} on T5. A clear differentiation between pCO_2 treatments was seen after T3, with Chl-*a* concentrations higher in the high pCO_2 treatment until the beginning of phase 2 at T9, after which they dropped below the Chl-*a* concentrations of the control and medium pCO_2 mesocosms. During the phase 2 nutrient-induced bloom after T14, Chl-*a* concentrations were lower at high pCO_2, and peaked around T19-T20, before declining through phase 3 until the end of the experiment. Several different phytoplankton species were significant contributors to the total Chl-*a* throughout the experiment as measured by HPLC pigment data, including diatoms (~35%), cryptophytes (~22%), chlorophytes (~20%) and haptophytes (~19%; Figure 4b). Other taxa, including cyanobacteria, dinoflagellates and chrysophytes made a minor (<4%) contribution to the total Chl-

a. Haptophyte equivalent Chl-*a* showed a peak in all pCO_2 treatments during phase 1, with maximum concentrations of 0.84 µg L^{-1} in the control mesocosms, and there were no significant differences between any treatments during this phase (F=0.73, p=0.669, n=98). The phase 1 haptophyte equivalent Chl-*a* was coincident with the peak in $DMSP_T$ concentrations (Figure 5b). The difference between elevated pCO_2 treatments became more apparent after the initial bloom (T7 to T17) and after the nutrient induced bloom in phase 2 (T22 to T29), with significantly lower haptophyte equivalent Chl-*a* concentrations in the higher pCO_2 treatments (F=16.74, p<0.01, n=189) from T9 compared to the low and medium pCO_2 mesocosms. During the period T3 to T10, mean net growth rates for the haptophytes in the three high pCO_2 mesocosms (1400-3000 µatm) were -0.2 d^{-1}, compared to the mean net growth rate in the low pCO_2 mesocosms (280-390 µatm) at -0.06 d^{-1}. Haptophyte growth rates during the artificial bloom in phase 2 were subsequently higher in the high pCO_2 mesocosms over the period T10 to T20 at 0.1 d^{-1} compared to 0.02 d^{-1} in the low pCO_2 mesocosms and 0.06 d^{-1} in the medium (540-1120 µatm) mesocosms, but overall haptophyte Chl-*a* remained lower throughout phase 2 into phase 3. The mean calculated percentage contribution of the haptophyte Chl-*a* to total Chl-*a* was 25 ± 11 % in the low pCO_2 mesocosms, but 15 ± 5 % in the highest, and this difference was pronounced in the post-bloom periods (Figure 4c).

Calcified (C-form) *E. huxleyi* was the only haptophyte to be identified and enumerated using flow cytometry (Figure 4d) however this method was not able to identify individual non-calcified haptophyte species; all these were combined in the small nanophytoplankton (2-6 µm) group with *E. huxleyi* (Figure 4e). Abundance of calcified *E. huxleyi* cells increased in abundance during phases 2 and 3 when the majority of other groups declined in abundance. *E. huxleyi* peaked on T29 in the control (280 µatm) at ~3000 cells mL^{-1}, and a distinct effect of pCO_2 treatment was observed, with significantly lower abundance in the high pCO_2 mesocosms (F=13.45, p<0.01, n=112). The nanophytoplankton group (2-6 µm) showed a similar pattern to the haptophyte equivalent Chl-*a* with a peak during each bloom period, but did not show significantly lower nanophytoplankton abundance at high pCO_2 during the post-bloom period of Phase 2 (T9-T15) directly following the initial bloom, which was notable in the haptophyte equivalent Chl-*a*. After T15, significantly lower cell abundance was identified in the in the highest pCO_2 mesocosms, yet higher abundance was seen in the in the medium pCO_2 mesocosms compared to the control. Net nanophytoplankton growth rates were comparable between all mesocosms for the period T5 to T15, in contrast to the haptophyte Chl-*a*, yet were lower in the high pCO_2 mesocosms during the period T15 to T20. Nanophytoplankton abundance ranged from ~3000 to 33500 cells mL^{-1} in all mesocosms, with maximum abundance in M8 (560 µatm) during Phase 2. Calcified *E. huxleyi* cells contributed less than 5% to the total nanophytoplankton during Phases 1 and 2 in all pCO_2 treatments, but increased in the low and medium pCO_2 treatments to 27 % at the end of Phase 3 (Figure 4f).

DMS

DMS concentrations were measured from T12 to T29 for the mesocosms only in phases 2 and 3 (Figure 5a). Until T19, DMS concentrations were below 1 nmol L^{-1} and from T20 onwards it increased in all pCO_2 treatments. A clear effect of increased pCO_2 is seen from the start of measurements on T12, with DMS concentrations in the highest pCO_2 treatments (2000 and 3000 µatm) significantly lower than the low (280 and 390 µatm) and medium pCO_2 (560, 840 and 1120 µatm) conditions ($F=5.52$, $p<0.01$, $n=175$), and these trends continued until T29. Maximum DMS concentrations were reached in M6 (390 µatm) on T29 at 4.9 nmol L^{-1}, compared to 0.76 nmol L^{-1} measured in M9 (3000 µatm) on T28. During phases 2 and 3, DMS concentrations in the high pCO_2 treatments were 60% lower than the control and the medium pCO_2 treatments 33% lower. Mean DMS concentrations plotted against the mean pCO_2 for phases 2 and 3 showed a clear decreasing relationship as pCO_2 increased (Figure 6a; $\rho=-0.595$, $p<0.01$, $n=140$), however with only three mesocosms at pCO_2 higher than 1000 µatm, it is difficult to determine the exact nature of the DMS/ pCO_2 relationship at these higher pCO_2.

Total DMSP

$DMSP_T$ was measured on alternate days from T-1 and showed different patterns to DMS (Figure 5b). $DMSP_T$ concentrations were similar in all treatments on T-1 (38.5 ± 4.3 nmol L^{-1} mean), and increased to a peak on T4, after which concentrations decreased. No difference between mesocosms was identified during phase 1 for $DMSP_T$ ($F=0.42$, $p=0.916$, $n=58$). A difference between mesocosms was more apparent for $DMSP_T$ during phases 2 and 3, with concentrations in the high (1400 – 3000 µatm) and medium pCO_2 treatments (560 – 1120 µatm) 32% and 14% lower respectively than the low pCO_2 mesocosms during both phases. This change seems to have been driven by the net DMSP production rate over the period T5 to T12, where the high pCO_2 mesocosms (1400-3000 µatm) showed a loss rate of -0.12 d^{-1} compared to the low pCO_2 mesocosms (280-390 µatm) at -0.04 d^{-1}. This higher loss rate, similar to that of the haptophyte equivalent Chl-*a*, influences the concentrations in the later part of phase 2 and during phase 3: $DMSP_T$ concentrations increased to a peak at T22 in all treatments, with the highest concentrations of 81.8 nmol L^{-1} in M1 (840 µatm) but the lowest at 26.3 nmol L^{-1} in M9 (3000 µatm). $DMSP_T$ concentrations then decreased at the start of phase 3, before increasing again in all treatments on T29, with the lowest concentrations measured in the highest pCO_2 treatments. A summary of the DMS, DMSP and relevant cell abundance is given in Table 1.

Relationships between DMS, DMSP and Biological Parameters

The community composition proxies (HPLC pigments and flow cytometry data) were analysed alongside the DMS and DMSP data to determine the potential sources of DMS and DMSP within the mesocosm communities. Using Spearman's Rank Correlation analysis, concentrations of DMS and $DMSP_T$ showed significant positive correlation to each other ($\rho=0.339$, $p<0.01$, $n=135$), and the ratio between the two compounds (Figure 5c) was relatively stable below 0.02 in all treatments during phase 2, but increased to around 0.06 in phase 3 corresponding to an increase in DMS concentration. The ratio of DMS: $DMSP_T$ was unaffected by CO_2 treatment: mean ratios were

plotted against mean pCO_2 in all mesocosms, and showed no change with increasing pCO_2 (Figure 6c; ρ=0.289, p=0.083, n=62).

$DMSP_T$ showed positive correlation with Chl-*a* (ρ=0.400, p<0.01, n=117), and an examination of the mean $DMSP_T$: Chl-a_{Hapto} ratio for each mesocosm plotted against mean pCO_2 for the entire experiment showed no effect of increased pCO_2 (Figure 6d; ρ=-0.01, p=0.920, n=99). DMS showed negative correlation with total Chl-*a* (ρ=-0.406, p<0.01, n=136). Correlations between DMS and all phytoplankton abundances and Chl-*a* contributors showed that DMS concentrations correlated only with the haptophyte-equivalent Chl-*a* (ρ=0.508, p<0.01, n=126) and calcified *E. huxleyi* abundance (ρ=0.615, p<0.01, n=136), however the latter only reached 3000 cells mL^{-1} in M4 (290 µatm) on T29 (Figure 4d). $DMSP_T$ correlation with haptophyte equivalent Chl-*a* was also strong (ρ=0.635, p<0.01, n=121), with relatively weak correlation with the nanophytoplankton (ρ=0.283, p<0.01, n=117) and no relationship with calcified *E. huxleyi* abundance. In addition, there was weak correlation between $DMSP_T$ and the diatoms (ρ=0.301, p<0.01, n=121). The ratios of DMS and $DMSP_T$ to nanophytoplankton (2-6 µm) abundance (Figures 7a and b) and haptophyte equivalent Chl-*a* (Figures 7c and d) were calculated on a daily basis, and showed a limited effect of elevated pCO_2. The haptophytes were significant contributors to the DMSP pool given the strong correlations with $DMSP_T$ and relatively high contribution to the total Chl-*a* (Figure 4c) while calcified *E. huxleyi* contributed to only a small percentage of the total haptophyte assemblage (Figure 4f) and subsequently the DMSP production. Calcified *E. huxleyi* were of greater importance to DMSP production during phase 3 of the experiment when the abundance was highest. It is highly likely that a large proportion of the nanophytoplankton (2-6 µm; Figure 4e) were non-calcified DMSP-producing haptophyte cells, although no determination of species composition could be made. Non-calcified *E. huxleyi* cannot be distinguished from other non-calcified haptophytes of the same size by flow cytometry (Aud Larsen, Pers. Comm.).

Discussion

A number of mesocosm experiments investigating the effect of elevated pCO_2 on the community structure have been performed, and several of these have measured the effects on DMS and DMSP concentrations. These are summarised in Table 2, alongside experiments on clonal *E. huxleyi* cultures which also measured DMS and DMSP versus CO_2 concentrations. The ranges in DMS and DMSP concentrations from the mesocosm experiment in this study are within those seen in previous Bergen mesocosm studies,[24,25,28,53,54] and the Korean and Svalbard mesocosm experiments, where microbial communities from neither location contained a significant abundance of *E. huxleyi*.[23,26,27] During this experiment no single group dominated the community at any time; there were high abundances of diatoms, cryptophytes, chlorophytes and haptophytes, but only the haptophytes were significantly correlated with DMSP concentrations. The pCO_2 range used by us was broader than in any previous investigation, with mesocosms at 2000 and 3000 µatm; the aim being to identify trends of different community parameters beyond the pCO_2 projected for the year 2100. The change in pCO_2 in the system occurred relatively rapidly over 3-5 days (Figure 3), and the community response would have favoured those species with less efficient carbon

concentrating mechanisms (CCMs), [55–57] as well as those better suited to rapid environmental change. Over the course of the experiment, the pCO_2 decreased in all the treated mesocosms, with the result that the artificial bloom was at a lower mean pCO_2 for each mesocosm than the initial bloom, but the communities would have been exposed to the perturbed conditions for a longer time period. Differences were identified between treatments for a number of community parameters: chlorophytes, picoeukaryotes and cyanobacteria showed a strong positive response in high pCO_2, while haptophyte and diatom growth was negatively affected at the highest pCO_2. These responses were more pronounced during the latter phases of the experiment.

Community Development and E. huxleyi Growth

The total Chl-*a* concentrations in the mesocosms showed both positive and negative effects of CO_2 during the three different phases, a scenario which was also identified during a mesocosm experiment in Svalbard[52], and is a result of different phytoplankton assemblages responding to elevated pCO_2 at different times of the experiment. Of importance to this investigation, haptophyte-equivalent Chl-*a*, nanophytoplankton and calcified *E. huxleyi* cells showed reduced abundance under increased pCO_2 during phases 2 and 3, either as a direct result of CO_2 on the groups, or as a result of differential nutrient-induced competition between groups such as diatoms and picoeukaryotes at the higher availability of DIC,[52,58,59] as was previously identified during the Svalbard mesocosm experiment in 2010. In contrast, Endres *et al.*[31] identified significantly higher marine bacterial abundance and activity in the high pCO_2 mesocosms during the same period. Calcified *E. huxleyi* cell counts during the mesocosm experiment were unexpectedly low (up to 3000 cells mL^{-1}) in comparison to some previous experiments (e.g. up to 70,000 cells mL^{-1} in Steinke *et al.*[53] and up to 50,000 cells mL^{-1} in Delille *et al.*[60]) and there was no analysis performed on calcification rates in *E. huxleyi* or evaluating coccolith formation. Analysis of the phytoplankton community by flow cytometry was unable to identify other calcified coccolithophore species than *E. huxleyi*, however the mismatch between the pattern of haptophyte equivalent Chl-*a* and the abundance of calcified *E. huxleyi* cells identified by flow cytometry indicate the presence of non-calcified haptophyte cells which were enumerated only as nanophytoplankton (2-6 µm). Previous investigations at Espegrend Marine Biological Station have identified non-calcified *E. huxleyi* cells within the coastal phytoplankton community.[61] Indeed, in a mesocosm experiment in the Raunefjord in 2008, a significant number (up to 40,000 cells mL^{-1}) of non-calcified haptophyte cells were identified in the natural population through the use of COD-FISH (combined $CaCO_3$ optical detection with fluorescent in-situ hybridisation) techniques.[62,63]

Calcification rates were not measured during our mesocosm and laboratory culture experiments, but previous mesocosm studies have identified reductions in calcification under elevated pCO_2,[60,64] which has been suggested as a negative feedback on surface water pCO_2.[10] As mentioned above, non-calcified *E. huxleyi* cells do occur in natural and mesocosm assemblages, but their presence is not indicative of lower calcification rates. Overall,

understanding of the non-calcified life-stages of *E. huxleyi* is very scant, and requires further investigation into the physiological changes that occur in the different forms (haploid and diploid, calcified and non-calcified). In addition, other non-calcifying haptophytes were likely present in the community and contributing to the haptophyte Chl-*a* signal. In terms of DMSP production, a single investigation found that DMSP production was increased by up to 0.4 pg cell^{-1} in a non-calcified *E. huxleyi* strain (N-Form diploid RCC1242) under 790 µatm pCO_2 compared to an ambient pCO_2 control, while a calcified strain (C-form diploid RCC1731) showed no CO_2 effect.[65] Further studies of DMSP production from diploid calcified and non-calcified (haploid and diploid) strains in the laboratory and non-calcified cells in the field are certainly warranted, as well as further investigation into the DMSP production of the haploid life-stages, which has never been previously investigated.

There have been a number of studies on the effect of elevated pCO_2 on different strains of *E. huxleyi*, isolated from different geographical areas,[9,65–70] but never using the strain RCC1229. This strain was chosen due to its origins in the North Sea close to the Bergen coast (58.42°N, 3.21°E), and likely similar genotype to the natural *E. huxleyi* identified during the Bergen mesocosm experiment. Despite this, calcified cell abundance in the mesocosms showed a significant decrease at 840 µatm pCO_2, but no such effect was identified during the culture experiments at the comparable pCO_2. While the culture experiments were nutrient replete, *E. huxleyi* within the mesocosms showed significant growth during phase 3 after the artificial bloom, when concentrations of inorganic nitrate and phosphate were low. Although RCC1229 was isolated close to the location of the mesocosm experiment, there is still likely significant genetic difference between the strain and the wild population. The physiological responses between different strains to increased pCO_2 have not been uniform: in general carbon fixation has increased, [65,68,70,71] but three strains investigated by Langer *et al.*[66] showed the opposite effect. *E. huxleyi* has shown varying sensitivity of growth rate to pCO_2 in the laboratory and the field. A previous mesocosm experiment identified decreased net specific growth rate from 0.5 d^{-1} to 0.43 d^{-1} in the highest pCO_2 mesocosms,[72] and the reduced haptophyte equivalent Chl-*a* concentrations and calcified *E. huxleyi* abundance values seen in our medium and high pCO_2 mesocosms support this. However, in the laboratory, varying responses have been identified for different *E. huxleyi* strains where growth rates either increased,[9,70,73] remained unchanged as in this study[65,69,74] or decreased.[66,75,76] Specific growth rates during the *E. huxleyi* RCC1229 experiment were lower (0.48 d^{-1} for the 900 µatm pCO_2 treatment and 0.47 d^{-1} for the ambient CO_2 control) than found previously for that strain under near-identical growth conditions at the same temperature (0.67 d^{-1}),[77] and was likely a result of methodological differences in culturing which can be a significant problem in comparing growth rates between different investigations. [78] The growth rate of calcified RCC1229 was not affected by 900 µatm pCO_2, whereas the abundance of calcified cells decreased in the 840 µatm pCO_2 mesocosm. A significant shift to a larger cell size was identified during the RCC1229 culture experiment, which reinforces the findings of Arnold *et al.*[69] using non-calcifying strain CCMP373, suggesting that the cell size increase is not linked to additional coccolith production. Increased POC production at higher pCO_2 has been linked to larger cell size. [79] The long-term studies of Lohbeck *et al.*[80] with over 500 generations of single and multi-clonal experiments found

a decrease in cell size as pCO_2 increased. These variations in growth rate and carbon fixation limit the use of a single *E. huxleyi* strain as a representative of all coccolithophores and haptophytes in the natural environment. In contrast, Franklin *et al.*[81] identified *E. huxleyi* as a good model for the coccolithophores as a whole, particularly in terms of DMSP production, but only examined two strains of *E. huxleyi*. Comparison of the experiments described here and existing studies on *E. huxleyi* suggest sufficient genetic diversity and plasticity in natural populations to at least partially adapt as surface water pCO_2 increases.[80] *E. huxleyi* has shown significant advancement into polar waters since the first half of the 20th century due to expansion of the thermal window,[82,83] but the effect of ocean acidification on these blooms is still unclear. Future laboratory high CO_2 experiments should focus on species other than *E. huxleyi*, and on other significant DMSP producers which would allow for better analysis of community development in mesocosm studies such as this.

DMS and DMSP

DMSP concentrations measured in the mesocosms were strongly correlated with haptophyte equivalent Chl-*a* and nanophytoplankton abundance, but not calcified *E. huxleyi* abundance. Although these groups were unlikely to be the sole producers of DMSP, the negative effect of acidification on the bloom dynamics of these groups had significant influence on the lower DMSP concentrations measured in the high pCO_2 mesocosms. DMSP correlated well with haptophyte Chl-*a*, with DMSP: Chl-a_{Hapto} ratios of 10-60 nmol μg^{-1} were in strong agreement with those identified in a previous mesocosm experiment.[28] During the period T9-T14, the increased DMSP: Chl-a_{Hapto} ratio in the high pCO_2 mesocosms was a result of the lower haptophyte Chl-*a*, likely due to nutrient competition, particularly with picoeukaryotes at the higher pCO_2 mesocosms during the natural post-bloom phase, and not a direct result of elevated pCO_2. The DMS: DMSP ratio was unaffected by the change in pCO_2 (Figure 6c), and therefore the reduction in DMSP would explain a proportion of the 60% reduction in DMS concentrations measured in the mesocosms. In a number of previous mesocosm experiments, measured DMS and DMSP concentrations were found to be negatively affected by increased pCO_2,[24,25,27] but in others the effect was either temporally offset,[28] or showed differential responses in DMS and DMSP.[23] While the $DMSP_T$ concentrations in the RCC1229 *E. huxleyi* experiment showed no significant difference between treatments, $DMSP_T$ was 12% lower in the 900 µatm pCO_2 treatment when normalised to cell volume (Figure 2d). In contrast, pH-stat laboratory experiments on clonal *E. huxleyi* cultures showed either no effect of elevated pCO_2, or increased DMSP production[65,69,84] when the pCO_2 was equivalent to that of our mid or high range mesocosm experiments (>800 µatm). DMS concentrations in the laboratory cultures showed no significant difference when normalised to cell volume, with no pronounced differences in *E. huxleyi* biomass, implying that microbial interaction occurs within the mesocosms which is limited in the cultures. Clearly, mesocosm experiments assess the community response to increasing pCO_2 whereas laboratory experiments investigate the physiological changes within a single species and the effect these have on the production of DMSP and DMS; the greater response to acidification in the mesocosms compared to the laboratory experiment implies that there is a strong community interaction in the

462 net production of DMS and DMSP. The DMSP producers showed no immediate DMSP-response upon addition of
463 the CO_2-enriched waters to the mesocosms (Figure 7b and d) over the T-1 to T3, implying that DMSP production is
464 not a direct response to changing environmental conditions.

465 The poor relationship of DMS with Chl-*a* has been reported several times, both regionally[85–87] and in data
466 analysis-global modelling studies[88], due to the likely differential DMSP synthesis of phytoplankton groups,
467 variability in community DMSP-to-DMS conversion yields, and DMS loss rate constants[89]. Total DMSP measured
468 in the mesocosms included the intracellular particulate DMSP ($DMSP_P$) and extracellular dissolved DMSP ($DMSP_D$).
469 DMS and $DMSP_T$ have often been found decoupled, particularly during the 'summer paradox' of delayed DMS
470 maxima compared to DMSP maxima and phytoplankton maximum abundance,[22,90,91] driven by grazing-induced
471 particulate DMSP transformation. DMSP is degraded through two separate pathways,[92]: demethylation to
472 methylmercaptopropionate (MMPA)[93] or cleavage to DMS with production of either acrylate or 3-
473 hydroxypropionate through the 'DMSP-Lyase' pathway,[92,94] and can be intracellular or extracellular by marine
474 bacteria in the surrounding waters.[95,96] These routes regulate the gross DMS production rates in seawater, and
475 thereby affect the flux of sulphur to the atmosphere. Previous studies on DMSP-lyase activity showed variations
476 in the pH optimum, from pH 5 in a number of haptophyte *Phaeocystis* spp. [97] and coccolithophore *Gephyrocapsa*
477 *oceanica*,[81] to pH 8 in the bacterium *Ruegeria lacuscaerulensis*[98] and *Pseudomonas doudoroffii* [99] and up to pH
478 10.5 in a further *Phaeocystis* strain.[100] The implication is that community production of DMS from the cleavage of
479 DMSP is unlikely to be immediately affected by lowered pH as a result of ocean acidification, but individual
480 species with optimal pH above 8 will find it increasingly difficult to cleave DMSP at higher atmospheric pCO_2.

481 The $DMSP_D$ pool supports 1-13% of bacterial carbon[18,101] and 3-100% of bacterial sulphur[18] demand, by the
482 breakdown pathways diverting sulphur away from DMS production.[102,103] Increased consumption of the $DMSP_D$
483 pool by bacteria would affect not only the $DMSP_T$ concentrations but also reduce DMS production from the
484 cleavage pathways. Bacterial transformation of DMS to DMSO has been identified as the removal pathway for the
485 majority of DMS,[104] further reducing the DMS concentrations during the greater bacterial activity at higher pCO_2.

486 In the laboratory experiments, bacterial abundance was kept low by treatment with antibiotics prior to the initial
487 inoculation, and were checked by DAPI staining at the end of the experiment, when bacterial abundances were
488 found to be low. During the mesocosm experiment, bacterial abundance increased by 28% in the high pCO_2
489 treatments in comparison to the low pCO_2 mesocosms, and showed three times higher leucine aminopeptidase
490 activity as a proxy for bacterial enzyme hydrolysis.[31] This higher bacterial abundance at high pCO_2 could result in
491 greater consumption of DMSP from the dissolved phase as a greater bacterial abundance and activity is likely to
492 drive an increased demand for sulphur sources, as well as drive greater conversion of DMS to DMSO. Bacterial
493 loss processes for both DMS and DMSP could account for the lower concentrations of both compounds at
494 elevated pCO_2, while not affecting the DMS: DMSP ratio.

During phase 3 of the experiment, there was an increase in DMS concentration which was not explained by corresponding increases in $DMSP_T$ (Figure 5c), haptophyte Chl-*a* (Figure 7c) or nanophytoplankton abundance (Figure 7a), but which was unaffected by elevated pCO_2 (Figure 6c) and implied that DMS turnover and loss processes were similar in all mesocosms. A study by Pinhassi *et al.*[105] in microcosms identified that DMSP was utilised as a sulphur source and removed by bacterioplankton more during the bloom phase (i.e. phase 2) than during senescence (i.e. phase 3), potentially resulting in greater availability of $DMSP_D$ during phase 3 for conversion to DMS. Scarratt *et al.*[106] identified a direct relationship of DMS concentrations with $DMSP_D$ in short-term incubations, which would imply a greater contribution of dissolved DMSP to the measured $DMSP_T$ in phase 3 of the mesocosm experiment, after the artificial nutrient-induced bloom in phase 2.

Summary

A significant reduction in DMS and DMSP concentrations was identified during a mesocosm experiment designed to study the effects of elevated pCO_2 on a coastal phytoplankton community. The major DMSP producers were identified as nanophytoplanktonic haptophytes which showed lower biomass under elevated pCO_2. The same effect was not observed during laboratory culture experiments on a calcifying strain of *E. huxleyi* (RCC1229), which indicates that consumption and turnover of $DMSP_D$ and DMS in surface waters at elevated pCO_2 by the microbial community is as important as gross DMSP production in determining the concentrations of DMS and DMSP in (future) acidified waters. Elevated pCO_2 affected the growth of calcified *E. huxleyi* and nanophytoplankton (2-6 µm) which would have contained non-calcified haptophyte cells, and the reduction in abundance significantly contributed to the lower DMSP concentrations at high pCO_2.

A number of mesocosm studies, including this one, have shown that the phytoplankton community response to an increase in pCO_2 has resulted in lower DMS concentrations than seen in the ambient pCO_2 concentrations of today.[1] This response is representative for the exposure of the current phytoplankton community assemblage to a comparatively rapid increase in pCO_2, and does not reflect the adaptation likely to occur in phytoplankton communities with the gradual increase in pCO_2 over the next 100 years. A reduction in DMS concentration will affect the atmospheric flux of sulphur from the marine environment. As many of these mesocosm experiments have been performed in a single location in Norway, further large-scale mesocosm experiments should be performed in different oceanic regions, to assess the changes in the parameters measured here for different microbial communities. Further investigations should concentrate on rates of DMSP production and the bacterial consumption of DMS and DMSP to develop a better understanding of the interactions with the microbial community that affect the concentrations of these compounds. DMS and DMSP analyses should also be included in long term (500+ generations) algal culture experiments, to establish if the short-term changes identified here are retained over a longer study period.

Acknowledgements

The Bergen 2011 mesocosm experiment was part of the SOPRAN (Surface Ocean Processes in the Anthropocene; 03F0611C) 2 Programme funded by the German Ministry for Education and Research (BMBF) and led by the GEOMAR Helmholtz Centre for Ocean Research Kiel, Germany. The authors thank all participants in the SOPRAN Bergen experiment for their assistance. Special thanks to A. Ludwig for logistical support, J. Czerny, L. Bach and M. Meyerhöfer for discussions of the trace gas data and J. R. Bermudez for analysis of samples by light microscopy. The staff at the Espegrend Marine Biological Station in Bergen, Norway, are acknowledged for their logistical support, in particular A. Aadnesen. We also thank R. Utting and A. Dimond for the support in the laboratory at the University of East Anglia.

This work was funded by a UK Natural Environment Research Council Directed Research Studentship (NE/H025588/1) through the UK Ocean Acidification Research Programme, with CASE funding from Plymouth Marine Laboratory. Additional funding was provided by the MINOS project funded by EU-ERC (project no. 250254).

We would like to thank the three anonymous reviewers for their comments on improving this manuscript.

References

[1] D.L. Hartmann, A.M.G. Klein Tank, M. Rusticucci, L.V. Alexander, S. Bronnimann, Y. Charabi, *et al.*, in: *Climate Change 2013: The Physical Science Basis. Contribution of Working Group 1 to the Fifth Assessment Report of the Intergovernmental Panel on Climate Change* (Eds T.F. Stocker, D. Qin, G.-K. Plattner, M. Tignor, S.K. Allen, J. Boschung, *et al.*) **2013**, (Cambridge University Press, Cambridge: Cambridge, UK.).

[2] U. Cubasch, D. Wuebbles, D. Chen, M.C. Facchini, D. Frame, N. Mahowald, *et al.*, in: *Climate Change 2013: The Physical Science Basis. Contribution of Working Group 1 to the Fifth Assessment Report of the Intergovernmental Panel on Climate Change* (Eds T.. Stocker, D. Qin, G.-K. Plattner, M. Tignor, S.K. Allen, J. Boschung, *et al.*) **2013**, (Cambridge University Press: Cambridge, UK.).

[3] C. Le Quéré, G.P. Peters, R.J. Andres, R.M. Andrew, T.A. Boden, P. Ciais, *et al.*, Global carbon budget 2013. *Earth Syst. Sci. Data* **2014**,*6*,235–263.

[4] R.A. Feely, S.C. Doney, S.R. Cooley, Ocean Acidification: present conditions and future changes in a high CO_2 world. *Oceanography* **2009**,*22*,36–47.

[5] J.C. Orr, V.J. Fabry, O. Aumont, L. Bopp, S.C. Doney, R.A. Feely, *et al.*, Anthropogenic ocean acidification over the twenty-first century and its impact on calcifying organisms. *Nature* **2005**,*437*,681–686.

[6] P.M. Holligan, M. Viollier, D.S. Harbour, P. Camus, M. Champagne-Phillipe, Satellite and ship studies of coccolithophore production along a continental shelf edge. *Nature* **1983**,*304*,339–342.

[7] P.M. Holligan, E. Fernandez, J. Aiken, W.M. Balch, P. Boyd, P.H. Burkill, *et al.*, A biogeochemical study of the coccolithophore *Emiliania huxleyi* in the North Atlantic. *Global Biogeochem. Cycles* **1993**,*7*,879–900.

[8] U. Riebesell, I. Zondervan, B. Rost, P.D. Tortell, R.E. Zeebe, F.M.M. Morel, Reduced calcification of marine plankton in response to increased atmospheric CO_2. *Nature* **2000**,*407*,364–367.

[9] A. Sciandra, J. Harlay, D. Lefèvre, R. Lemée, P. Rimmelin, M. Denis, *et al.*, Response of coccolithophorid *Emiliania huxleyi* to elevated partial pressure of CO_2 under nitrogen limitation. *Mar. Ecol. Prog. Ser.* **2003**,*261*,111–122.

[10] I. Zondervan, R.E. Zeebe, B. Rost, U. Riebesell, Decreasing marine biogenic calcification: a negative feedback on rising pCO_2. *Global Biogeochem. Cycles* **2001**,*15*,507–516.

[11] H. Elderfield, Carbonate mysteries. *Science (80-.).* **2002**,*296*,1618–1621.

[12] A. Vairavamurthy, M.O. Andreae, R.L. Iverson, Biosynthesis of dimethylsulfide and dimethylpropiothetin by *Hymenomonas carterae* in relation to sulfur source and salinity variations. *Limnol. Oceanogr.* **1985**,*30*,59–70.

[13] M. Levasseur, Impact of Arctic meltdown on microbial cycling of sulphur. *Nat. Geosci.* **2013**,*6*,691–700.

[14] W. Sunda, D.J. Kieber, R.P. Kiene, S. Huntsman, An antioxidant function for DMSP and DMS in marine algae. *Nature* **2002**,*418*,317–320.

[15] S. Strom, G. Wolfe, J. Holmes, H. Stecher, C. Shimeneck, S. Lambert, *et al.*, Chemical defense in the microplankton I: Feeding and growth rates of heterotrophic protists on the DMS-producing phytoplankter *Emiliania huxleyi*. *Limnol. Oceanogr.* **2003**,*48*,217–229.

[16] J.R. Seymour, R. Simó, T. Ahmed, R. Stocker, Chemoattraction to dimethylsulfoniopropionate throughout the marine microbial food web. *Science* **2010**,*329*,342–345.

[17] M. Garren, K. Son, J.-B. Raina, R. Rusconi, F. Menolascina, O.H. Shapiro, *et al.*, A bacterial pathogen uses dimethylsulfoniopropionate as a cue to target heat-stressed corals. *ISME J.* **2014**,*8*,999–1007.

[18] R. Simó, M. Vila-Costa, L. Alonso-Sáez, C. Cardelús, Ó. Guadayol, E. Vázquez-Dominguez, *et al.*, Annual DMSP contribution to S and C fluxes through phytoplankton and bacterioplankton in a NW Mediterranean coastal site. *Aquat. Microb. Ecol.* **2009**,*57*,43–55.

[19] M. Vila-Costa, R. Simó, H. Harada, J.M. Gasol, D. Slezak, R.P. Kiene, Dimethylsulfoniopropionate uptake by marine phytoplankton. *Science* **2006**,*314*,652–654.

[20] R.J. Charlson, J.E. Lovelock, M.O. Andreae, S.G. Warren, Oceanic phytoplankton, atmospheric sulphur, cloud albedo and climate. *Nature* **1987**,*326*,655–661.

[21] P.K. Quinn, T.S. Bates, The case against climate regulation via oceanic phytoplankton sulphur emissions. *Nature* **2011**,*480*,51–56.

[22] A. Lana, T.G. Bell, R. Simó, S.M. Vallina, J. Ballabrera-Poy, A.J. Kettle, *et al.*, An updated climatology of surface dimethlysulfide concentrations and emission fluxes in the global ocean. *Global Biogeochem. Cycles* **2011**,*25*.

[23] S.D. Archer, S.A. Kimmance, J.A. Stephens, F.E. Hopkins, R.G.J. Bellerby, K.G. Schulz, *et al.*, Contrasting responses of DMS and DMSP to ocean acidification in Arctic waters. *Biogeosciences* **2013**,*10*,1893–1908.

[24] F.E. Hopkins, S.M. Turner, P.D. Nightingale, M. Steinke, D. Bakker, P.S. Liss, Ocean acidification and marine trace gas emissions. *Proc. Natl. Acad. Sci. U. S. A.* **2010**,*107*,760–765.

[25] V. Avgoustidi, P.D. Nightingale, I. Joint, M. Steinke, S.M. Turner, F.E. Hopkins, *et al.*, Decreased marine dimethyl sulfide production under elevated CO_2 levels in mesocosm and in vitro studies. *Environ. Chem.* **2012**,*9*,399–404.

[26] J.-M. Kim, K. Lee, E.J. Yang, K. Shin, J.H. Noh, K.-T. Park, *et al.*, Enhanced production of oceanic dimethylsulfide resulting from CO_2-induced grazing activity in a high CO_2 world. *Environ. Sci. Technol.* **2010**,*44*,8140–8143.

[27] K.-T. Park, K. Lee, K. Shin, E.J. Yang, B. Hyun, J.-M. Kim, *et al.*, Direct linkage between dimethyl sulfide production and microzooplankton grazing, resulting from prey composition change under high partial pressure of carbon dioxide conditions. *Environ. Sci. Technol.* **2014**,*48*,4750–4756.

[28] M. Vogt, M. Steinke, S.M. Turner, A. Paulino, M. Meyerhöfer, U. Riebesell, *et al.*, Dynamics of dimethylsulphoniopropionate and dimethylsulphide under different CO_2 concentrations during a mesocosm experiment. *Biogeosciences* **2008**,*5*,407–419.

[29] F.E. Hopkins, S.D. Archer, Consistent increase in dimethyl sulphide (DMS) in response to high CO_2 in five shipboard bioassays from contrasting NW European waters. *Biogeosciences* **2014**,*11*,4925–4940.

[30] J. Piontek, C. Borchard, M. Sperling, K.G. Schulz, U. Riebesell, A. Engel, Response of bacterioplankton activity in an Arctic fjord system to elevated pCO_2: results from a mesocosm perturbation study. *Biogeosciences* **2013**,*10*,297–314.

[31] S. Endres, L. Galgani, U. Riebesell, K.-G. Schulz, A. Engel, Stimulated bacterial growth under elevated pCO_2: results from an off-shore mesocosm study. *PLoS One* **2014**,*9*,e99228.

[32] R.A. Andersen, J.A. Berges, P.J. Harrison, M.M. Watanabe, *Algal culturing techniques*. **2005** (Imprint Academic Press)

[33] N. Jaeckisch, I. Yang, S. Wohlrab, G. Glöckner, J. Kroymann, H. Vogel, *et al.*, Comparative genomic and transcriptomic characterization of the toxigenic marine dinoflagellate *Alexandrium ostenfeldii. PLoS One* **2011**,*6*,e28012.

[34] A.G. Dickson, The measurement of sea water pH. *Mar. Chem.* **1993**,*44*,131–142.

[35] A.G. Dickson, The carbon dioxide system in seawater: equilibrium chemistry and measurements. in: *Guide to Best Practices for ocean acidification research and data reporting* (Ed. Riebesell, U., Fabry, V. J., Hannson, L. and Gatuso, J.-P.) **2010**, pp. 17–40. Publications Office of the European Union: Luxembourg.

[36] National Measurement Institute of Australia, *Proficiency Study 12-23: DMS in seawater*. **2013**

[37] U. Riebesell, J. Czerny, K. von Bröckel, T. Boxhammer, J. Büdenbender, M. Deckelnick, *et al.*, Technical Note: A mobile sea-going mesocosm system – new opportunities for ocean change research. *Biogeosciences* **2013**,*10*,1835–1847.

[38] K.G. Schulz, J. Barcelos e Ramos, R.E. Zeebe, U. Riebesell, CO_2 perturbation experiments: similarities and differences between dissolved inorganic carbon and total alkalinity manipulations. *Biogeosciences* **2009**,*6*,2145–2153.

[39] K.. Johnson, J.M. Sieburth, P.J. le B. Williams, L. Brändström, Coulometric total carbon dioxide analysis for marine studies: automation and calibration. *Mar. Chem.* **1987**,*21*,117–133.

[40] A.G. Dickson, C.L. Sabine, J.R. Christian, Guide to best practices for ocean CO_2 measurements. *PICES Spec. Publ.* **2007**,*3*.

[41] C. Mehrbach, C.H. Culberson, J.E. Hawley, R.M. Pytkowicz, Measurement of the apparent dissociation constants of carbonic acid in seawater at atmospheric pressure. *Limnol. Oceanogr.* **1973**,*18*,897–907.

[42] T.J. Lueker, A.G. Dickson, C.D. Keeling, Ocean pCO_2 calculated from dissolved inorganic carbon, alkalinity, and equations for K1 and K2: Validation based on laboratory measurements of CO_2 in gas and seawater at equilibrium. *Mar. Chem.* **2000**,*70*,105–119.

[43] A.L. Chuck, S.M. Turner, P.S. Liss, Oceanic distributions and air-sea fluxes of biogenic halocarbons in the open ocean. *J. Geophys. Res.* **2005**,*110*.

[44] C. Hughes, G. Malin, P.D. Nightingale, P.S. Liss, The effect of light stress on the release of volatile iodocarbons by three species of marine microalgae. *Limnol. Oceanogr.* **2006**,*51*,2849–2854.

[45] M. Martino, P.S. Liss, J.M.C. Plane, The photolysis of dihalomethanes in surface seawater. *Environ. Sci. Technol.* **2005**,*39*,7097–7101.

[46] M.A.J. Curran, G.B. Jones, H. Burton, Spatial distribution of dimethylsulfide and dimethylsulfoniopropionate in the Australasian sector of the Southern Ocean. *J. Geophys. Res.* **1998**,*103*,16677–16689.

[47] R.P. Kiene, D. Slezak, Low dissolved DMSP concentrations in seawater revealed by small-volume gravity filtration and dialysis sampling. *Limnol. Oceanogr. Methods* **2006**,*4*,80–95.

[48] A. Larsen, T. Castberg, R.A. Sandaa, C.P.D. Brussaard, J. Egge, M. Heldal, *et al.*, Population dynamics and diversity of phytoplankton, bacteria and viruses in a seawater enclosure. *Mar. Ecol. Prog. Ser.* **2001**,*221*,47–57.

[49] N.A. Welschmeyer, Fluorometric analysis of chlorophyll a in the presence of chlorophyll b and pheopigments. *Limnol. Oceanogr.* **1994**,*39*,1985–1992.

[50] R.G. Barlow, D.G. Cummings, S.W. Gibb, Improved resolution of mono- and divinyl chlorophylls a and b and zeaxanthin and lutein in phytoplankton extracts using reverse phase C-8 HPLC. *Mar. Ecol. Prog. Ser.* **1997**,*161*,303–307.

[51] M.D. Mackey, D.J. Mackey, H.W. Higgins, S.W. Wright, CHEMTAX a program for estimating class abundances from chemical markers: application to HPLC measurements of phytoplankton. *Mar. Ecol. Prog. Ser.* **1996**,*144*,265–283.

[52] K.G. Schulz, R.G.J. Bellerby, C.P.D. Brussaard, J. Büdenbender, J. Czerny, A. Engel, *et al.*, Temporal biomass dynamics of an Arctic plankton bloom in response to increasing levels of atmospheric carbon dioxide. *Biogeosciences* **2013**,*10*,161–180.

[53] M. Steinke, C. Evans, G.A. Lee, G. Malin, Substrate kinetics of DMSP-lyases in axenic cultures and mesocosm populations of *Emiliania huxleyi*. *Aquat. Sci.* **2007**,*69*,352–359.

[54] M. Levasseur, S. Michaud, J. Egge, G. Cantin, J.C. Nejstgaard, R. Sanders, *et al.*, Production of DMSP and DMS during a mesocosm study of an *Emiliania huxleyi* bloom: influence of bacteria and *Calanus finmarchicus* grazing. *Mar. Biol.* **1996**,*126*,609–618.

671 [55] M. Hein, K. Sand-Jensen, CO_2 increases oceanic primary production. *Nature* **1997**,*388*,526–527.

672 [56] B. Rost, U. Riebesell, S. Burkhardt, D. Sultemeyer, Carbon acquisition of bloom-forming marine
673 phytoplankton. *Limnol. Oceanogr.* **2003**,*48*,55–67.

674 [57] B. Rost, I. Zondervan, D. Wolf-Gladrow, Sensitivity of phytoplankton to future changes in ocean carbonate
675 chemistry: current knowledge, contradictions and research directions. *Mar. Ecol. Prog. Ser.* **2008**,*373*,227–
676 237.

677 [58] C.P.D. Brussaard, A.A.M. Noordeloos, H. Witte, M.C.J. Collenteur, K. Schulz, A. Ludwig, *et al.*, Arctic
678 microbial community dynamics influenced by elevated CO_2 levels. *Biogeosciences* **2013**,*10*,719–731.

679 [59] Y. Wu, D.A. Campbell, A.J. Irwin, D.J. Suggett, Z. V Finkel, Ocean acidification enhances the growth rate of
680 larger diatoms. *Limnol. Oceanogr.* **2014**,*59*,1027–1034.

681 [60] B. Delille, J. Harlay, I. Zondervan, S. Jacquet, L. Chou, R. Wollast, *et al.*, Response of primary production and
682 calcification to changes of pCO_2 during experimental blooms of the coccolithophorid *Emiliania huxleyi*.
683 *Global Biogeochem. Cycles* **2005**,*19*,GB2023.

684 [61] B.S.C. Leadbeater, Identification, by means of electron microscopy, of flagellate nanoplankton from the
685 coast of Norway. *Sarsia* **1972**,*49*,107–124.

686 [62] S. Jacquet, M. Heldal, M.D. Iglesias-Rodriguez, A. Larsen, W. Wilson, G. Bratbak, Flow cytometric analysis of
687 an *Emiliania huxleyi* bloom terminated by viral infection. *Aquat. Microb. Ecol.* **2002**,*27*,111–124.

688 [63] M.J. Frada, K.D. Bidle, I. Probert, C. de Vargas, In situ survey of life cycle phases of the coccolithophore
689 *Emiliania huxleyi* (Haptophyta). *Environ. Microbiol.* **2012**,*14*,1558–1569.

690 [64] Y. Feng, C.E. Hare, K. Leblanc, J.M. Rose, Y. Zhang, G.R. DiTullio, *et al.*, Effects of increased pCO_2 and
691 temperature on the North Atlantic spring bloom. I. The phytoplankton community and biogeochemical
692 response. *Mar. Ecol. Prog. Ser.* **2009**,*388*,13–25.

693 [65] A. Spielmeyer, G. Pohnert, Influence of temperature and elevated carbon dioxide on the production of
694 dimethylsulfoniopropionate and glycine betaine by marine phytoplankton. *Mar. Environ. Res.* **2012**,*73*,62–
695 69.

696 [66] G. Langer, G. Nehrke, I. Probert, J. Ly, P. Ziveri, Strain-specific responses of *Emiliania huxleyi* to changing
697 seawater carbonate chemistry. *Biogeosciences* **2009**,*6*,2637–2646.

698 [67] N.A. Nimer, M.J. Merrett, Calcification rate in *Emiliania huxleyi* Lohmann in response to light, nitrate and
699 availability of inorganic carbon. *New Phytol.* **1993**,*123*,673–677.

700 [68] K.T. Lohbeck, U. Riebesell, S. Collins, T.B.H. Reusch, Functional genetic divergence in high CO_2 adapted
701 *Emiliania huxleyi* populations. *Evolution (N. Y).* **2012**,*67*,1892–1900.

702 [69] H.E. Arnold, P. Kerrison, M. Steinke, Interacting effects of ocean acidification and warming on growth and
703 DMS-production in the haptophyte coccolithophore *Emiliania huxleyi*. *Glob. Chang. Biol.* **2013**,*19*,1007–
704 1016.

705 [70] D. Shi, Y. Xu, F.M.M. Morel, Effects of the pH/pCO_2 control method on medium chemistry and
706 phytoplankton growth. *Biogeosciences* **2009**,*6*,1199–1207.

[71] N.A. Nimer, M.J. Merrett, Calcification and utilization of inorganic carbon by the coccolithophorid *Emiliania huxleyi* Lohmann. *New Phytol.* **1992**,*121*,173–177.

[72] A. Engel, I. Zondervan, K. Aerts, L. Beaufort, A. Benthien, L. Chou, *et al.*, Testing the direct effect of CO_2 concentration on a bloom of the coccolithophorid *Emiliania huxleyi* in mesocosm experiments. *Limnol. Oceanogr.* **2005**,*50*,493–507.

[73] L.F. Dong, N.A. Nimer, E. Okus, M.J. Merrett, Dissolved inorganic carbon utilization in relation to calcite production in *Emiliania huxleyi* (Lohmann) Kamptner. *New Phytol.* **1993**,*123*,679–684.

[74] D.M. Kottmeier, S.D. Rokitta, P.D. Tortell, B. Rost, Strong shift from HCO_3^- to CO_2 uptake in *Emiliania huxleyi* with acidification: new approach unravels acclimation versus short-term pH effects. *Photosynth. Res.* **2014**,*121*,265–275.

[75] M.D. Iglesias-Rodriguez, P.R. Halloran, R.E.M. Rickaby, I.R. Hall, E. Colmenero-Hidalgo, J.R. Gittins, *et al.*, Phytoplankton calcification in a high-CO_2 world. *Science (80-.).* **2008**,*320*,336–340.

[76] J. Barcelos e Ramos, M.N. Müller, U. Riebesell, Short-term response of the coccolithophore *Emiliania huxleyi* to an abrupt change in seawater carbon dioxide concentrations. *Biogeosciences* **2010**,*7*,177–186.

[77] M. Heinle, The effects of light, temperature and nutrients on coccolithophores and implications for biogeochemical models. *PhD Thesis, Univ. East Angl.* **2013**,

[78] P.W. Boyd, T.A. Rynearson, E.A. Armstrong, F. Fu, K. Hayashi, Z. Hu, *et al.*, Marine phytoplankton temperature versus growth responses from polar to tropical waters - outcome of a scientific community-wide study. *PLoS One* **2013**,*8*,e63091.

[79] M.N. Müller, K.G. Schulz, U. Riebesell, Effects of long-term high CO_2 exposure on two species of coccolithophores. *Biogeosciences* **2010**,*7*,1109–1116.

[80] K.T. Lohbeck, U. Riebesell, T.B.H. Reusch, Adaptive evolution of a key phytoplankton species to ocean acidification. *Nat. Geosci.* **2012**,*5*,346–351.

[81] D.J. Franklin, M. Steinke, J. Young, I. Probert, G. Malin, Dimethylsulphoniopropionate (DMSP), DMSP-lyase activity (DLA) and dimethylsulphide (DMS) in 10 species of coccolithophore. *Mar. Ecol. Prog. Ser.* **2010**,*410*,13–23.

[82] J.C. Cubillos, S.W. Wright, G. Nash, M.F. de Salas, B. Griffiths, B. Tilbrook, *et al.*, Calcification morphotypes of the coccolithophorid *Emiliania huxleyi* in the Southern Ocean: changes in 2001 to 2006 compared to historical data. *Mar. Ecol. Prog. Ser.* **2007**,*348*,47–54.

[83] A. Winter, J. Henderiks, L. Beaufort, R.E.M. Rickaby, C.W. Brown, Poleward expansion of the coccolithophore *Emiliania huxleyi*. *J. Plankton Res.* **2014**,*36*,316–325.

[84] T. Wuori, The effects of elevated pCO_2 in the physiology of *Emiliania huxleyi*. *Master's Thesis, West. Washingt. Univ.* **2012**,

[85] M.G. Scarratt, M. Levasseur, S. Michaud, S. Roy, DMSP and DMS in the Northwest Atlantic: Late-summer distributions, production rates and sea-air fluxes. *Aquat. Sci.* **2007**,*69*,292–304.

[86] C. Leck, U. Larsson, L.E. Bågander, S. Johansson, S. Hajdu, Dimethyl sulfide in the Baltic Sea: annual variability in relation to biological activity. *J. Geophys. Res.* **1990**,*95*,3353–3363.

[87] S.M. Turner, G. Malin, P.S. Liss, D.S. Harbour, P.M. Holligan, The seasonal variation of dimethyl sulfide and dimethylsulfoniopropionate concentrations in nearshore waters. *Limnol. Oceanogr.* **1988**,*33*,364–375.

[88] A. Lana, R. Simó, S.M. Vallina, J. Dachs, Re-examination of global emerging patterns of ocean DMS concentration. *Biogeochemistry* **2012**,*110*,173–182.

[89] P.S. Liss, A.D. Hatton, G. Malin, P.D. Nightingale, S.M. Turner, Marine sulphur emissions. *Philos. Trans. R. Soc. B Biol. Sci.* **1997**,*352*,159–169.

[90] M. Galí, R. Simó, A meta-analysis of oceanic DMS and DMSP cycling processes: Disentangling the summer paradox. *Global Biogeochem. Cycles* **2015**,*29*,496–515.

[91] R. Simó, C. Pedrós-Alió, Role of vertical mixing in controlling the oceanic production of dimethyl sulphide. *Nature* **1999**,*402*,396–398.

[92] A.R.J. Curson, J.D. Todd, M.J. Sullivan, A.W.B. Johnston, Catabolism of dimethylsulphoniopropionate: microorganisms, enzymes and genes. *Nat. Rev. Microbiol.* **2011**,*9*,849–859.

[93] E.C. Howard, J.R. Henriksen, A. Buchan, C.R. Reisch, H. Bürgmann, R. Welsh, *et al.*, Bacterial taxa that limit sulphur flux from the ocean. *Science (80-.).* **2006**,*314*,649–652.

[94] J.D. Todd, R. Rogers, Y.G. Li, M. Wexler, P.L. Bond, L. Sun, *et al.*, Structural and regulatory genes required to make the gas dimethyl sulfide in bacteria. *Science (80-.).* **2007**,*315*,666–669.

[95] E.C. Howard, S. Sun, C.R. Reisch, D.A. del Valle, H. Bürgmann, R.P. Kiene, *et al.*, Changes in dimethylsulfoniopropionate demethylase gene assemblages in response to an induced phytoplankton bloom. *Appl. Environ. Microbiol.* **2011**,*77*,524–531.

[96] M. Zubkov, L.J. Linn, R. Amann, R.P. Kiene, Temporal patterns of biological dimethylsulfide (DMS) consumption during laboratory-induced phytoplankton bloom cycles. *Mar. Ecol. Prog. Ser.* **2004**,*271*,77–86.

[97] B.R. Mohapatra, A.N. Rellinger, D.J. Kieber, R.P. Kiene, Kinetics of DMSP lyases in whole cell extracts of four Phaeocystis species: Response to temperature and DMSP analogs. *J. Sea Res.* **2014**,*86*,110–115.

[98] C.-Y. Li, T.-D. Wei, S.-H. Zhang, X.-L. Chen, X. Gao, P. Wang, *et al.*, Molecular insight into bacterial cleavage of oceanic dimethylsulfoniopropionate into dimethyl sulfide. *Proc. Natl. Acad. Sci. U. S. A.* **2014**,*111*,1026–1031.

[99] M. De Souza, D. Yoch, Comparative physiology of dimethyl sulfide production by dimethylsulfoniopropionate lyase in *Pseudomonas doudoroffii* and *Alcaligenes* sp. Strain M3A. *Appl. Environ. Microbiol.* **1995**,*61*,3986–3991.

[100] J. Stefels, L. Dijkhuizen, Characteristics of DMSP-lyase in *Phaeocystis* sp.(Prymnesiophyceae). *Mar. Ecol. Prog. Ser.* **1996**,*131*,307–313.

[101] R.P. Kiene, L.J. Linn, J.A. Bruton, New and important roles for DMSP in marine microbial communities. *J. Sea Res.* **2000**,*43*,209–224.

[102] M. Vila-Costa, D.A. del Valle, J.M. González, D. Slezak, R.P. Kiene, O. Sánchez, *et al.*, Phylogenetic identification and metabolism of marine dimethylsulfide-consuming bacteria. *Environ. Microbiol.* **2006**,*8*,2189–2200.

[103] H. Schäfer, Isolation of Methylophaga spp. from marine dimethylsulfide-degrading enrichment cultures and identification of polypeptides induced during growth on dimethylsulfide. *Appl. Environ. Microbiol.* **2007**,*73*,2580–2591.

[104] A.D. Hatton, D.M. Shenoy, M.C. Hart, A. Mogg, D.H. Green, Metabolism of DMSP, DMS and DMSO by the cultivable bacterial community associated with the DMSP-producing dinoflagellate *Scrippsiella trochoidea*. *Biogeochemistry* **2012**,*110*,131–146.

[105] J. Pinhassi, R. Simó, J.M. González, M. Vila, L. Alonso-Saez, R.P. Kiene, *et al.*, Dimethylsulfoniopropionate turnover is linked to the composition and dynamics of the bacterioplankton assemblage during a microcosm phytoplankton bloom. *Appl. Environ. Microbiol.* **2005**,*71*,7650–7660.

[106] M.G. Scarratt, M. Levasseur, S. Schultes, S. Michaud, G. Cantin, A. Vezina, *et al.*, Production and consumption of dimethylsulfide (DMS) in North Atlantic waters. *Mar. Ecol. Prog. Ser.* **2000**,*204*,13–26.

Table 1. Comparison of *E. huxleyi* cell counts and DMS and $DMSP_T$ concentration ranges and means for the mesocosm and the *E. huxleyi* culture experiments. All *E. huxleyi* counts show calcified cells only. The % changes in total measured DMS and $DMSP_T$ concentrations are also shown. NS: Not significant

Experiment	***E. huxleyi* RCC1229 Culture Experiment**		**Mesocosm Experiment**		
pCO_2 treatment	390 µatm	900 µatm	390 µatm	840 µatm	3000 µatm
E. huxleyi range (cells mL^{-1})	87439 – 1355000	60598 – 1254000	81 – 2004	58 – 1393	15 – 135
Nanophytoplankton (2-6µm) range (cells mL^{-1})			2341 – 28628	2373 – 29412	2453 – 20649
DMS range (nmol L^{-1})	6.5 – 345.8	11.5 – 366.6	0.4 – 4.9	0.1 – 2.4	0.1 – 0.8
DMS Mean (±SD) (nmol L^{-1})	74.5 ± 73.7	77.8 ± 83.4	1.5 ± 1.2	1.0 ± 0.6	0.4 ± 0.2
DMS % Change		NS		-17	-60
$DMSP_T$ range (nmol L^{-1})	109.8 – 6233.6	144.1 – 6062.3	21.1 – 67.4	20.3 – 81.9	14.6 – 58.2
$DMSP_T$ Mean (±SD) (nmol L^{-1})	1840.2 ± 1621.1	1769.0 ± 1546.5	46.0 ± 12.0	44.5 ± 15.6	28.8 ± 15.2
$DMSP_T$ % Change		NS		-13	-32

799 **Table 2. Comparison of DMS and DMSP concentrations from this study and previous pCO_2 perturbation experiments. ND –**
800 **not detected, NC – No change. * indicates concentrations were given in mmol DMSP L^{-1}.**

	Location or Culture Strain	pCO_2 Range (µatm)	Range DMS (nmol L^{-1})	% change DMS	Range DMSP (nmol L^{-1})	% change DMSP	Author
Bergen Mesocosm Experiment, 2011	Raunesfjorden, Norway	280 – 3000	0.09 – 4.92	-60	14.3 – 88.2	-32	This Study
Korean Mesocosm Experiment 2, 2012	Jangmok, Korea	160 - 830	1.0 - 100	-82	10-350	-71	Park *et al.* 2014[27]
EPOCA Svalbard, 2010	Kongsfjorden, Svalbard	180 - 1420	ND - 14	-60	ND-80	+50	Archer *et al.* 2013[23]
Korean Mesocosm Experiment 1, 2008	Jangmok, Korea	400 - 900	1 - 12	+80	No Data	No Data	Kim *et al.* 2010[26]
NERC Microbial Metagenomics Experiment, 2006	Raunesfjorden, Norway	300-750	ND - 50	-57	30 - 500	-24	Hopkins *et al.* 2010[24]
PeECE III, 2005	Raunesfjorden, Norway	300 - 750	ND - 35	NC	10 - 500	NC	Vogt *et al.* 2008[28]
PeECE II, 2003	Raunesfjorden, Norway	300 - 750	3 - 30	-40	ND - 300	-40	Avgoustidi *et al.* 2012[25]
UKOA European Shelf Cruise, 2011	NW European Shelf	340 - 1000	0.5 - 12	+225	5 - 80	-52	Hopkins and Archer 2014[71]
***E. huxleyi* Batch Experiments**	CCMP1516	370 - 760	0.1 – 2.5	-90	500 - 4000	-60	Avgoustidi *et al.* 2012[25]
***E. huxleyi* pH stat experiment**	CCMP 373	385 - 1000	2.5 – 5.0	NC	84.0 – 200	NC	Arnold *et al.* 2013[69]
***E. huxleyi* Semi-continuous Experiment**	RCC1242	390 - 790			100 – 270*	+30	Spielmeyer and Pohnert 2012[65]
***E. huxleyi* Semi-continuous Experiment**	RCC1731	390 – 790			50-60*	NC	

801

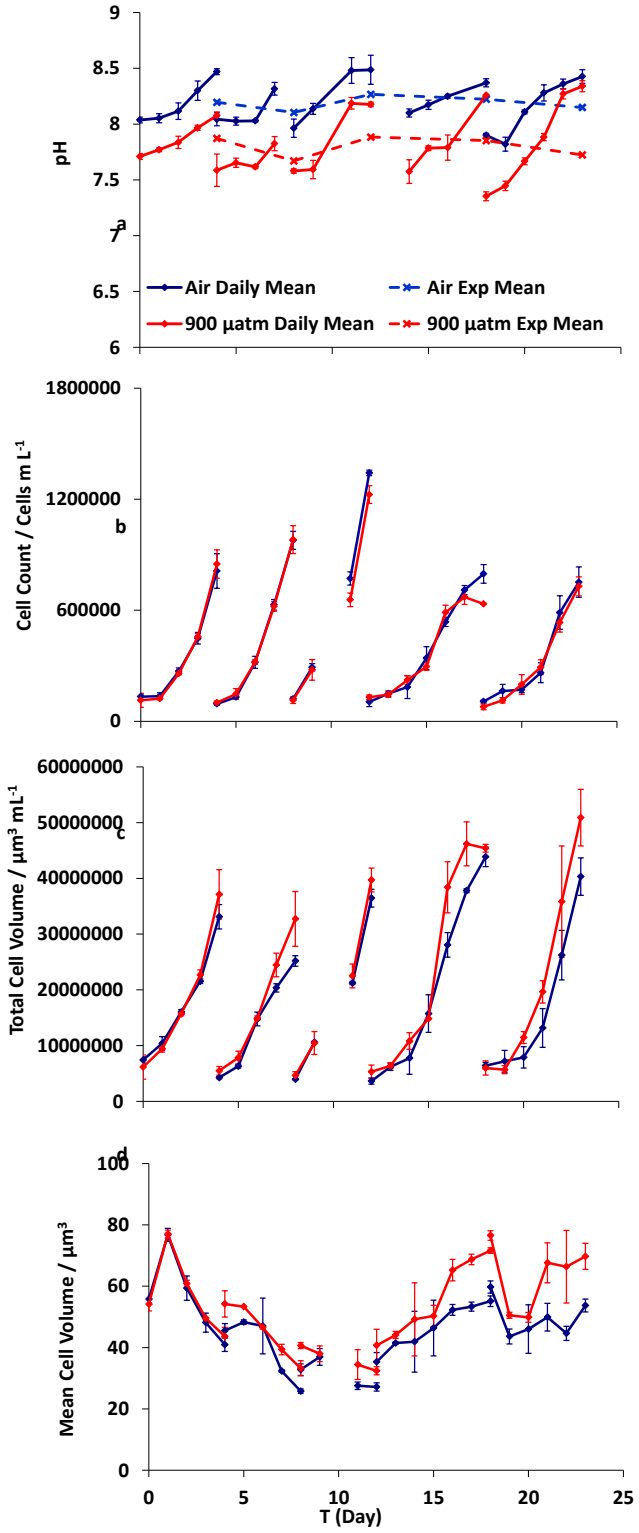

Figure 1. Growth dynamics of the 900 µatm pCO_2 (red) and control (blue) cultures showing the mean and standard deviation as error bars for three replicate flasks for (a) pH, (b) cell count (cells mL^{-1}), (c) total cell volume (μm^3 mL^{-1}) and (d) individual cell volume (μm^3). Dashed lines for pH show the mean pH for each inoculation period across the duration of the experiment.

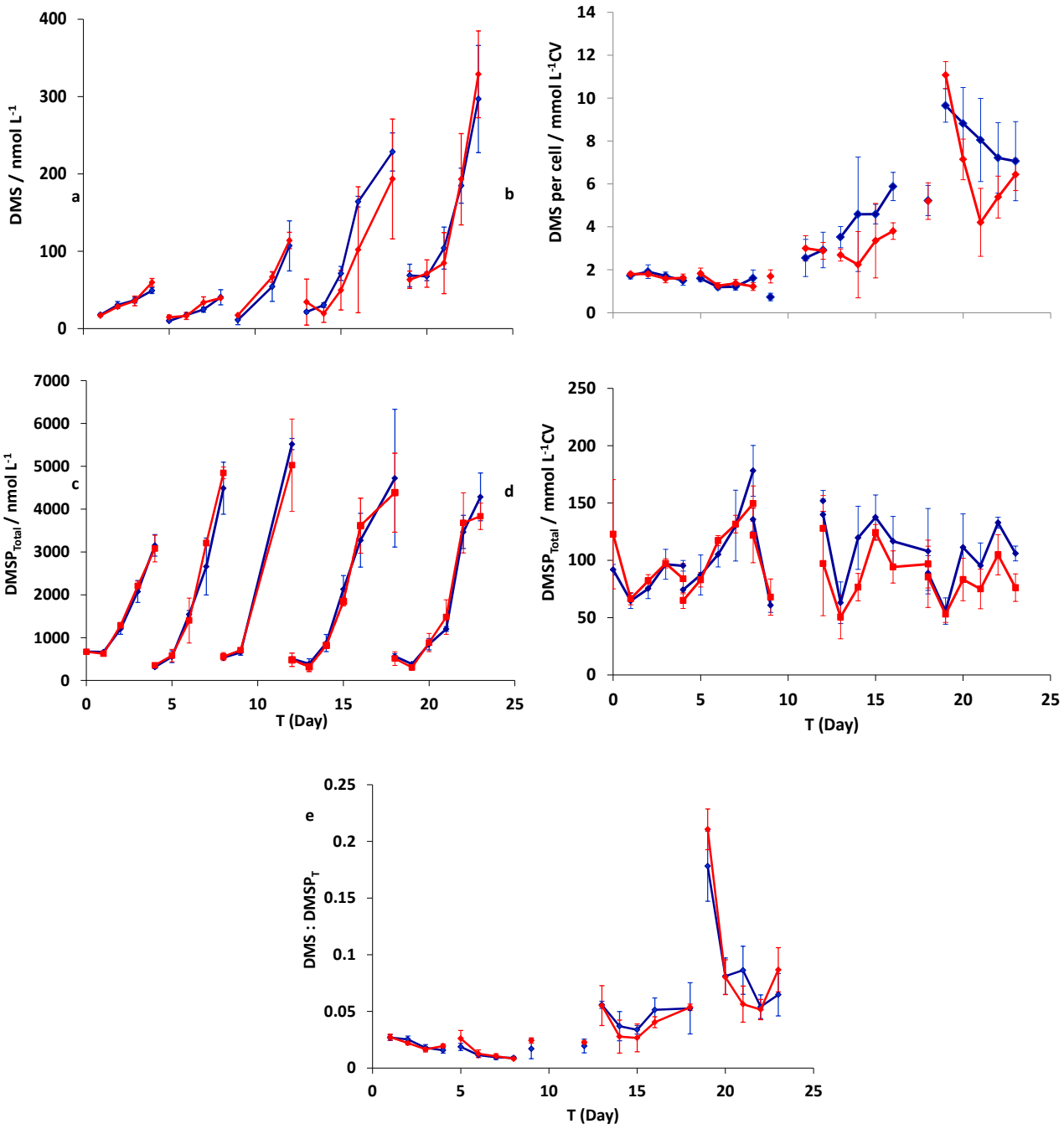

Figure 2. DMS and DMSP dynamics of the 900 µatm pCO_2 (red) and control (blue) treatments, showing the mean and standard deviation as error bars of three replicate flasks for each treatment. (a) DMS concentration (nmol L^{-1}), (b) DMS normalised to cell volume (mmol L^{-1} CV), (c) $DMSP_T$ concentration (nmol L^{-1}), (d) $DMSP_T$ normalised to cell volume (mmol L^{-1} CV) and (e) DMS: DMSP ratio.

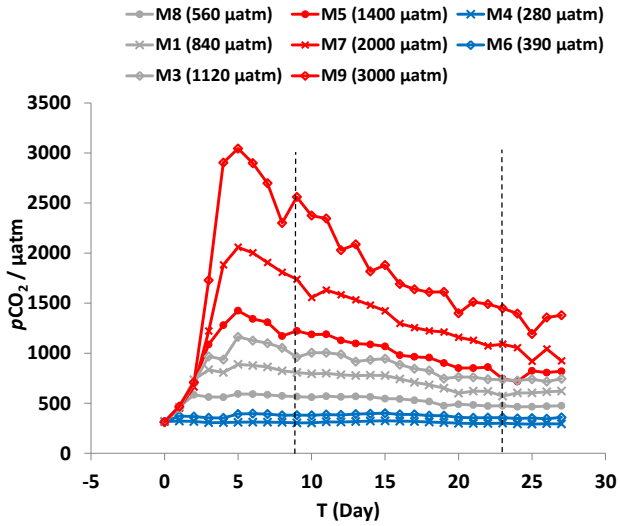

Figure 3. Daily measurements of pCO_2 during the mesocosm experiment. Dashed lines indicate the three phases of the experiment: the initial bloom, the second bloom and the post-bloom phase. Blue lines indicate the low pCO_2 (280 – 390 µatm), grey lines the mid-range pCO_2 (560 – 1120 µatm) and red lines the high pCO_2 (1400 – 3000 µatm).

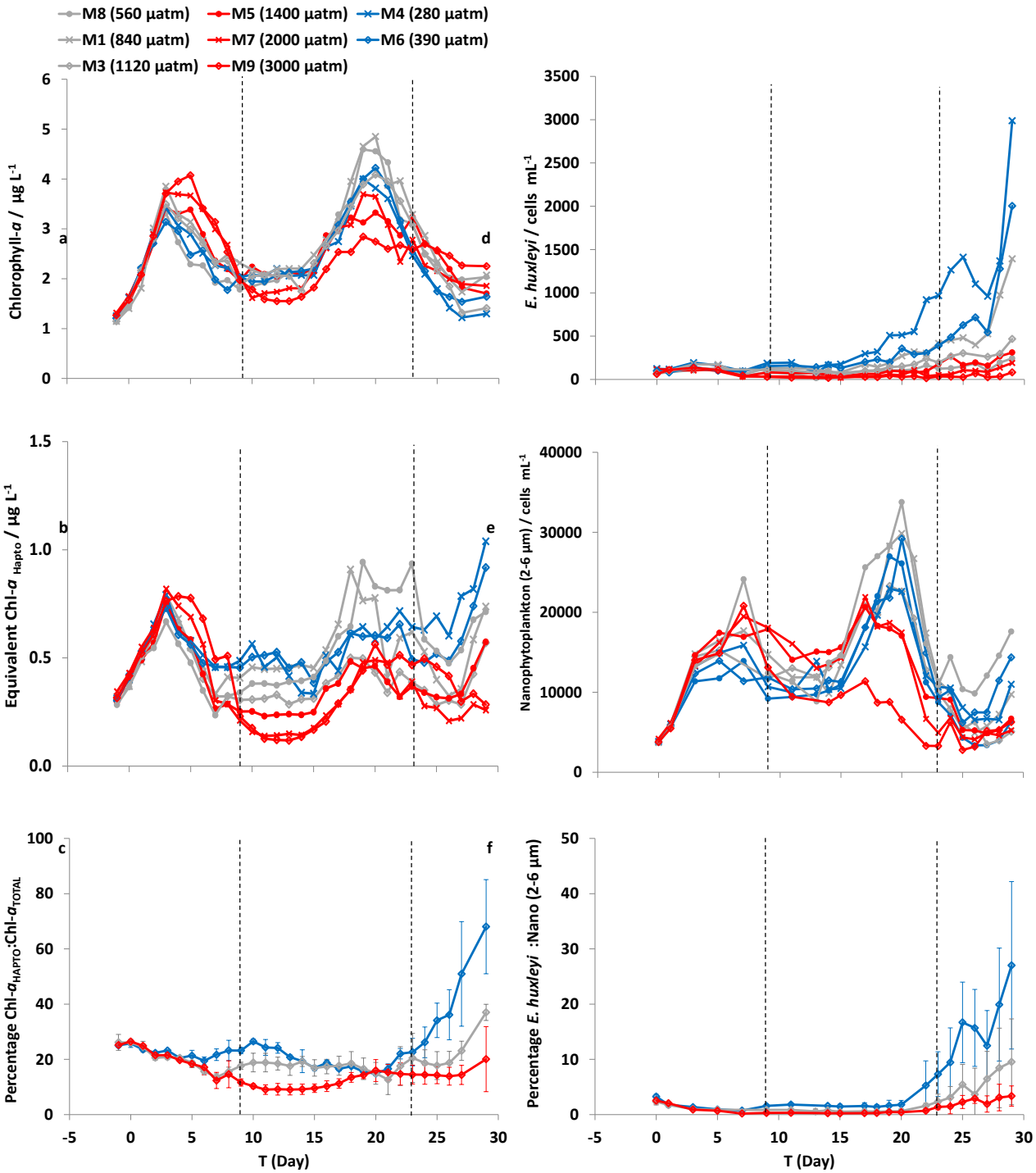

Figure 4. Temporal changes in (a) Chl-*a* (µg L^{-1}), (b) haptophyte equivalent Chl-*a* (µg L^{-1}), (c) percentage haptophyte Chl-*a*: total Chl-*a*, (d) calcified *E. huxleyi* cell abundance (cells mL^{-1}), (e) small nanophytoplankton including *E. huxleyi* (2-6 µm; cells mL^{-1}) and (f) percentage *E. huxleyi*: small nanophytoplankton during the mesocosm experiment. Dashed lines indicate the three phases of the experiment: the initial bloom, the second bloom and the post-bloom phase. Blue lines indicate the low (280 – 390 µatm), grey lines the mid-range pCO_2 (560 – 1120 µatm) and red lines the high pCO_2 (1400 – 3000 µatm). Error bars show the standard deviation between all mesocosms of low, medium and high pCO_2.

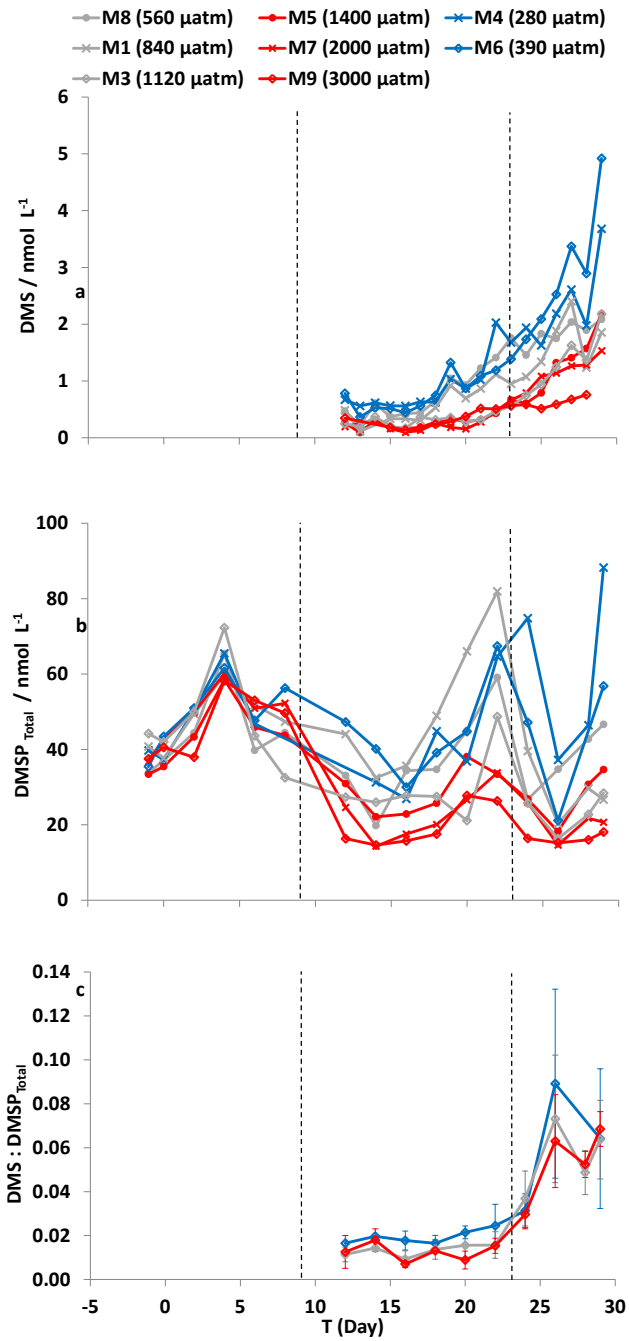

Figure 5. Temporal changes in (a) DMS (nmol L^{-1}) and (b) $DMSP_T$ (nmol L^{-1}) with a single analysis per treatment. Blue lines indicate the low pCO_2 treatments (280 – 390 µatm), grey lines the mid-range pCO_2 treatments (560 – 1120 µatm) and red lines the high pCO_2 treatments (1400 – 3000 µatm). The DMS: $DMSP_T$ ratio was calculated during Phases 2 and 3 of the experiment (c) with error bars showing the standard deviation between all mesocosms of low, medium and high pCO_2. Dashed lines indicate the three phases of the experiment.

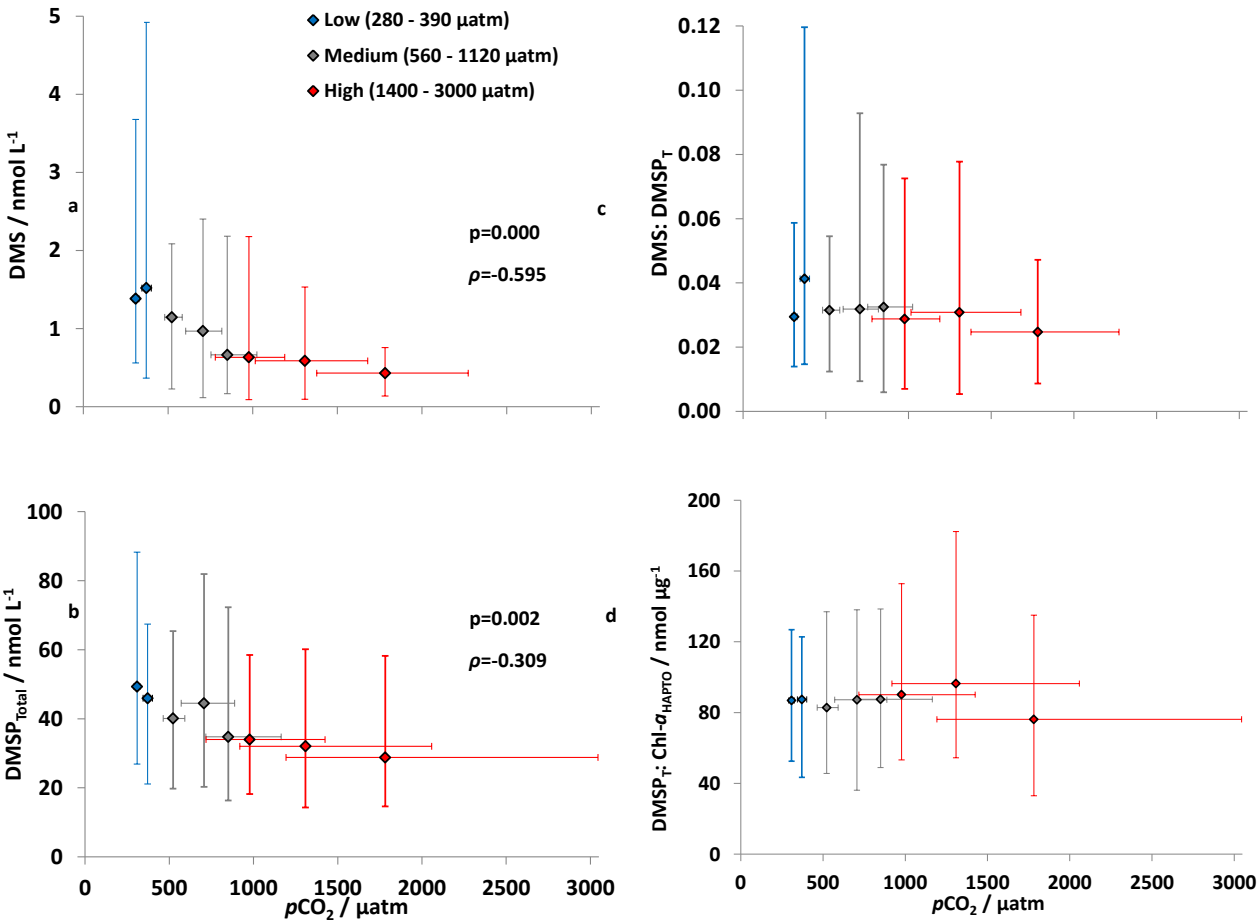

Figure 6. Relationships between pCO_2 and (a) mean DMS concentration (nmol L^{-1}) (b) mean $DMSP_T$ concentration (nmol L^{-1}) (c) mean DMS:$DMSP_T$ and (d) mean $DMSP_T$: Chl-*a* (nmol μg^{-1}) for the low (blue; 280 – 390 µatm), medium (grey; 540 – 1120 µatm) and high (red; 1400 – 3000 µatm) pCO_2 treatments, plotted against the mean pCO_2 in each mesocosm. Error bars show the range of the data on the horizontal and vertical axes. Where significant, the Spearman's Rank Correlation Coefficients (ρ) for the relationships between the variables are shown, with the corresponding p-value.

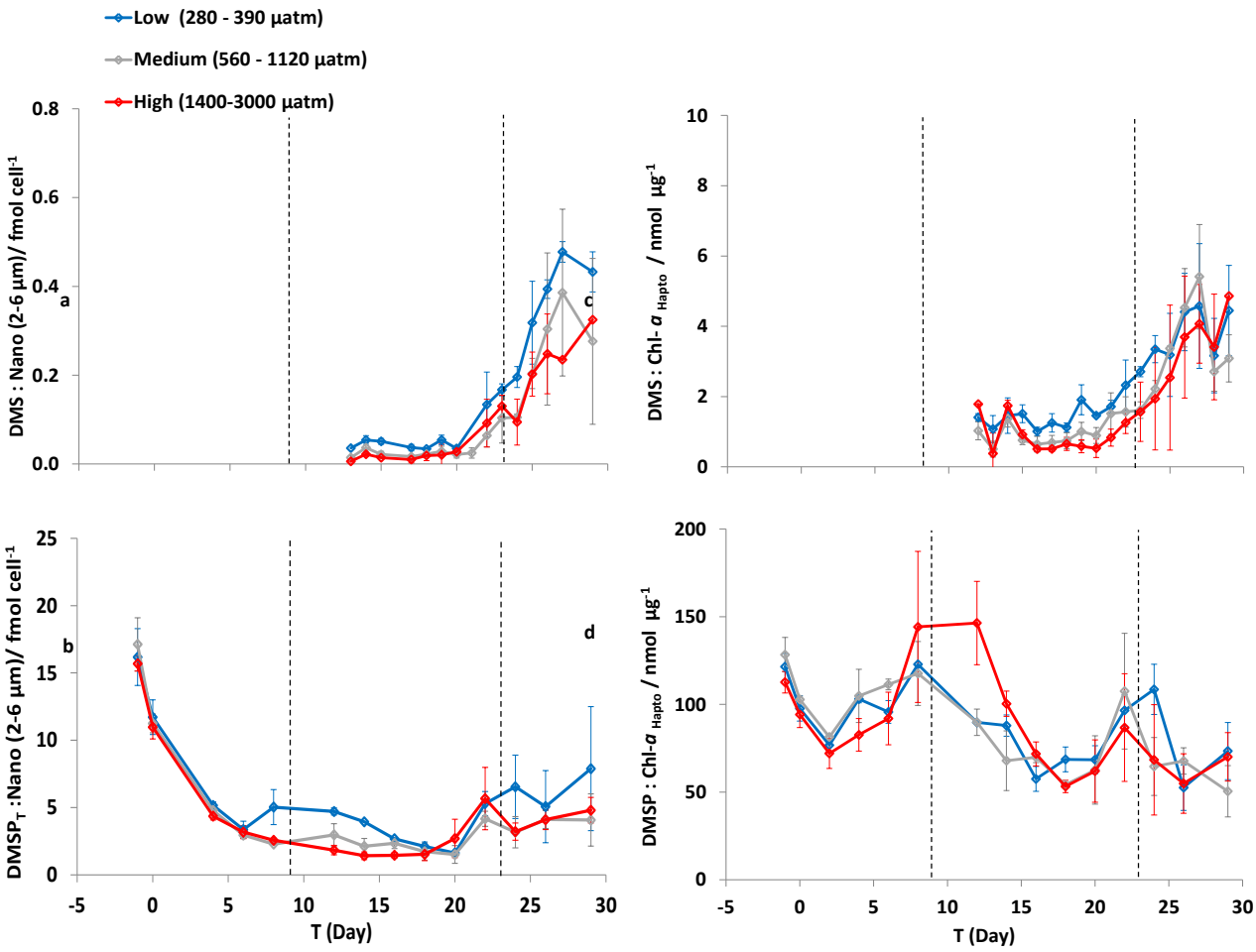

Figure 7. Mean ratios of (a) DMS to nanophytoplankton (2-6µm) (fmol cell^{-1}), (b) DMSP$_T$ to nanophytoplankton (2-6µm) including *E. huxleyi* (fmol cell^{-1}) (c) DMS to haptophyte equivalent Chl-*a* (nmol ug^{-1}), and (d) DMSP$_T$ to haptophyte equivalent Chl-*a* (nmol ug^{-1}) for three different *p*CO$_2$ conditions: low (blue; 280 µatm), medium (grey; 390 – 1120 µatm) and high (red; 1400 – 3000 µatm). Error bars show the standard deviation between all mesocosms of low, medium and high *p*CO$_2$.